Genomic regions of current low hybridisation mark long-term barriers to gene flow in scarce swallowtail butterflies

Sam Ebdon*, [1], Dominik R. Laetsch[1], Roger Vila[2], Stuart J.E. Baird[3, †], and Konrad Lohse[1, †]

[1]Institute of Ecology and Evolution, University of Edinburgh, Edinburgh, EH9 3FL, UK

[2]Institut de Biologia Evolutiva (CSIC-Universitat Pompeu Fabra), Passeig Marítim de la Barceloneta 37, ESP-08003, Barcelona, Spain

[3]Institute of Vertebrate Biology, Academy of Sciences of the Czech Republic, Brno, Czech Republic

∗ Corresponding author: se13@sanger.ac.uk

† These authors contributed equally to this work

Abstract

Many closely related species continue to hybridise after millions of generations of divergence. However, the extent to which current patterning in hybrid zones connects back to the speciation process remains unclear: does evidence for current multilocus barriers support the hypothesis of speciation due to multilocus divergence? We analyse whole-genome sequencing data to investigate the speciation history of the scarce swallowtails *Iphiclides podalirius* and *I. feisthamelii*, which abut at a narrow (∼25 km) contact zone north of the Pyrenees. We first quantify the heterogeneity of effective migration rate under a model of isolation with migration, using genomes sampled across the range to identify long-term barriers to gene flow. Secondly, we investigate the recent ancestry of individuals from the hybrid zone using genome polarisation and estimate the coupling coefficient under a model of a multilocus barrier. We infer a low rate of long-term gene flow from *I. feisthamelii* into *I. podalirius* the direction of which matches the admixture across the hybrid zone and complete reproductive isolation across ≈ 33% of the genome. Our contrast of recent and long-term gene flow shows that regions of low recent hybridisation are indeed enriched for long-term barriers which maintain divergence between these hybridising sister

species. This paves the way for future analysis of the evolution of reproductive isolation along the speciation continuum.

Author summary

Efforts to understand how new species evolve typically approach the problem through either: 1) investigating patterns of genetic exchange across 'hybrid zones' — where closely related species interbreed — or 2) modelling the demographic history of closely related species. Both approaches are capable of quantifying variation in genetic exchange, or 'gene flow', along the genome to identify regions of reproductive isolation; yet they leverage genetic signatures across vastly different timescales. The former exploits very recent signatures, while the latter averages long-term signatures over the history of divergence. Hence, we can contrast the genomic distribution of barriers acting on these very different timescales to test how patterns of gene flow change across the speciation continuum. Here we use this strategy to capture the speciation dynamics of a pair of hybridising papilionid butterflies. Our results show that not only are these species continuing to produce hybrids after more than a million years since the onset of divergence, but there is a significant degree of concordance between patterns of gene flow observed along the genome across time scales.

Introduction

A fundamental goal of speciation research is to understand the genetic basis of reproductive isolation (RI) between diverging species and quantify the demographic and selective processes that lead to a build-up of RI (Campbell et al., 2018). We now know that speciation in the face of gene flow is not only possible (Bush, 1994; Dieckmann and Doebeli, 1999; Nosil, 2008; Feder et al., 2012) but frequent (Taylor et al., 2001; Wang et al., 1997; Martin et al., 2013; Roux et al., 2016; Taylor and Larson, 2019): closely related species often continue to hybridise after millions of generations of divergence (Mallet, 1986; Harrison et al., 1990; Rieseberg et al., 1999; Sankararaman et al., 2014), yet remain distinct despite low levels of gene flow (Stankowski et al., 2021). However, given the time scales over which speciation events develop, the processes that contribute to RI are likely to vary over time (Drès and Mallet, 2002). Stankowski and Ravinet (2021) define the speciation continuum as a continuum of reproductive isolation, from incipience to complete hybrid inviability, and highlight that the species we observe today are at different stages along this continuum. For example, sister species in many temperate plant and animal taxa form secondary contact zones (Hewitt, 1988; Remington, 1968) which may be substantially younger than the onset of speciation. In other words, contemporary contact zones are likely one of many instances of secondary contact

generated by drastic environmental changes, such as glacial cycles over the last 800,000 years (Ebdon et al., 2021). Hybrid zones (HZs) for such taxa are stable exactly because there is strong selection against admixed ancestry. Whilst it is evident that genetic divergence and differentiation varies along the genome (Grainger Hunt and Selander, 1973; Nosil et al., 2009), understanding the extent to which this reflects variation in the rate of gene flow requires explicit modelling of the interplay between migration, selection, genetic drift, and recombination.

Locally beneficial alleles may be selected against if they migrate into unfavourable environments and/or genetic backgrounds, reducing effective gene flow (Lenormand, 2002). Over time, gene flow may vary as a consequence of range shifts and/or other changes in demography caused by glacial cycles, and – as a consequence – the selective forces and targets underpinning RI may also vary over time. Periods of complete allopatry during which gene flow is interrupted facilitate the build-up of strong endogeneous (Kruuk et al., 1999) or 'intrinsic' barriers (Bank et al., 2012). Genetic studies of HZs show that recent introgression may vary considerably along the genome (Payseur and Rieseberg, 2016): some genome regions harbouring strong incompatibilities act as strong barriers and show steep clines (Barton and Bengtsson, 1986; Yang et al., 2020). Steep clines in nature predicted (Macholán et al., 2011) the approximate location of the second mammalian hybrid sterility gene Hstx2 years before its identification in the lab (Bhattacharyya et al., 2014). In other regions introgression may be unimpeded by selection or even advantageous (Hedrick, 2013; Arnold et al., 2008; Racimo et al., 2015). Importantly, the barriers associated with RI since the onset of divergence may differ from those acting during secondary contact, many of which may have arisen recently (Abbott et al., 2013; Ravinet et al., 2017). To date, very few studies have compared the targets of short-term selection against heterospecific ancestry in hybrids with barriers to gene flow measured over different timescales. A recent meta-analysis of barriers to gene flow between the Western and Eastern European house mouse (*Mus musculus domesticus* vs *M. musculus musculus*) found no significant overlap between postzygotic incompatibilities mapped in interspecific crosses in the lab and barriers to gene flow detected in the natural HZ of these taxa (Frayer and Payseur, 2024). There are biological reasons for the non-repeatability between barriers detected in lab studies and HZs: firstly, the former are heavily biased towards barriers acting in the F1 or the first few backcross generations, the formation of which is extremely unlikely in natural HZs (which are typically several dispersal distances wide). Secondly, as argued by Frayer and Payseur (2024) "the loci underlying barriers observed in the lab may be distinct from those that impede gene flow in nature" and may be involved in pre-mating isolation and/or extrinsic local adaptation. However, the lack of overlap found by Frayer and Payseur (2024) may simply reflect a lack of statistical

power resulting from the fact that their study pooled information from many clinal analyses with varying (but high) false positive rates and that mapping studies have low resolution in general; an n-generation lab cross study can only generate $O(n)$ crossovers per chromosome.

Thus, one may argue that contrasts of HZ (short-term) barriers with barriers acting over the longer term are not only more biologically relevant than contrasts with lab-based (early generation) hybrids, but also have greater statistical power, at least in principle. This simply reflects the fact that a typical HZ individual involves a much larger number of admixture generations, ancestors, and junctions in ancestry than any lab-cross. However, previous attempts to investigate the overlap of HZ introgression with long-term barriers relied on comparing outliers of genetic differentiation with cline-based analyses and yielded mixed results: while several systems show strong associations between divergence and introgression (Gompert and Buerkle, 2012; Gosset and Bierne, 2013; Taylor et al., 2014; Yang et al., 2020), numerous other case studies revealed considerable heterogeneity (Teeter et al., 2008; Parchman et al., 2013; Kingston et al., 2017; Westram et al., 2021). In practice, comparisons between HZ and outliers of genetic differentiation have been limited for two reasons: firstly, summary statistics of the site frequency spectrum (such as F_{ST}) confound the effect of long-term barriers with other population genetic processes and, by focusing on the most extreme outliers, limit sample size and power. Secondly the power of clinal analyses has been limited by the need for extensive geographic sampling (which is impossible and/or prohibitively expensive for many natural HZ systems) and insufficiency of summary statistics; e.g. clines are often merely centered and scaled without allowing for variation in their shape and asymmetry.

The lack of comparisons of barriers to gene flow across recent and long-term timescales has been highlighted in a recent review on speciation genomics (Ravinet et al., 2017). However, filling this gap requires quantitative inference frameworks that can distinguish barriers on both time scales from other evolutionary processes using the limited sample sizes available for most natural HZs. Such approaches have only become available recently.

Speciation in *Iphiclides* butterflies

The southern European 'scarce swallowtails' *Iphiclides podalirius* and *I. feisthamelii* are large papilionid butterflies, typically associated with various species of *Prunus* and other Rosaceae bushes and trees. While *I. podalirius* ranges across the north of the Mediterranean from France to East Asia, *I. feisthamelii* is restricted to the Iberian peninsula and the northwest of Africa (Fig 1). Despite a long appreciation of the phenotypic differences between the two species (Godart, 1842), including

genital morphology (Coutsis and Van Oorschot, 2011) and male ultraviolet wing patterns (Gaunet et al., 2019), their taxonomic status has been disputed after DNA barcoding at the mitochondrial (*mt*) *COX1* locus revealed that the two taxa share *mt* haplotypes (Wiemers, 2003; Wiemers and Fiedler, 2007). However, it has been suggested recently that the *mt* genealogy reflects an introgression sweep most likely linked to infection by *Wolbachia* (Gaunet et al., 2019). The two taxa diverged approximately 1.2 million years ago (Wiemers and Gottsberger, 2010; Ebdon et al., 2021) and today, the species abut at a narrow (∼25 km) contact zone north of the Pyrenees (Descimon and Mallet, 2009) (Fig 1). While potential hybrids have been diagnosed based on morphology in a small set of museum specimens from France (Lafranchis et al., 2015), the putative HZ has not yet been characterised genetically. Here, we quantify introgression across the HZ and estimate long-term effective migration rates (m_e) for this pair of sister species.

Aims and objectives

We investigate the history of speciation and quantify both long and short-term barriers between *I. podalirius* and *I. feisthamelii*. We use two recently developed minimal-assumption inference methods `gIMble` (Laetsch et al., 2023) and `diem` (Baird et al., 2023) on whole-genome sequencing (WGS) data to quantify long-term barriers and selection against recent introgression in the HZ, respectively. Firstly, we infer variation in the rate of long-term effective migration along the genome under an explicit demographic model and locate putative long-term barriers to gene flow with `gIMble`. Secondly, we use the genome polarisation framework `diem` to quantify recent introgression barriers using six putative hybrid individuals sampled from the *Iphiclides* HZ (Fig 1) and characterize the multilocus barrier to ongoing hybridisation between these species. Finally, we investigate the overlap between long-term barriers to gene flow and genomic regions that are depleted for recent introgression. We address the following questions:

1. What is the direction and rate of gene flow between *I. podalirius* and *I. feisthamelii* since their initial divergence?
2. What fraction of the *Iphiclides* genome acts as a long-term barrier to gene flow, and what are the properties of barrier regions?
3. What is the evidence for recent gene flow between the species across the HZ?
4. Is introgression across the HZ impeded by long-term barriers to gene flow, i.e. do the barriers acting over these two different timescales overlap?

5. What is the strength of the multilocus barrier acting against introgression in the HZ?

Results

Interspecific variation is consistent with hybridisation in *Iphiclides*

We generated WGS data for six individuals from the *Iphiclides* hybrid zone (we will refer to these as "the HZ set") in southern France (Fig 1 B) and 14 individuals sampled throughout the ranges of both species ("the non-HZ set", Fig 1 A). The non-HZ set includes six samples of *I. podalirius* and eight of *I. feisthamelii*.

Visualising genetic variation in a PCA reveals distinct clusters both within and between species. The first principle component (PC1) captures interspecies differentiation between *I. podalirius* and *I. feisthamelii* ($\approx 23\%$ of the variation, Fig 2). Samples assigned morphologically to each species form two clusters along PC1 with individuals from the HZ (Fig 2) falling between the two parental species clusters (Fig 2). The North African *I. feisthamelii* samples are separated from the European *I. feisthamelii* samples along PC2 ($\approx 14\%$ of the variation, Fig 2). Genetic diversity is slightly larger in *I. feisthamelii* compared to *I. podalirius* (Table 1).

We identified runs of homozygosity (ROH) > 100kb using PLINK (v1.9) (Purcell et al., 2007) to estimate inbreeding via F_{ROH}. One *I. podalirius* sample from Sicily (RVcoll12R048) was particularly inbred ($F_{ROH} \approx 0.25$), and two other *I. podalirius* individuals, one from Romania (RVcoll14E561) and one from the HZ (1325) were somewhat inbred ($F_{ROH} \approx 0.076$ and 0.061 respectively). F_{ROH} in the remaining samples (including all *I. feisthamelii*) was negligible (see Supplementary Table 1).

An IM model supports a history of speciation with gene flow from *I. feisthamelii* into *I. podalirius*

We use the composite-likelihood method `gIMble` (Laetsch et al., 2023) to infer long-term barriers. This analytic framework co-estimates variation in long-term m_e along the genome. Contrasting the support for a background IM model and a history without gene flow in genomic windows gives a measure for the strength of putative barriers. Since this analysis of long-term barriers relies on the assumption of a two-population history, HZ and North African samples were excluded. We summarise genetic variation in short 64 base 'blocks', which are assumed to be non-recombining, under no direct selection, and to evolve with a constant mutation rate. These assumptions allow

Table 1 – Estimates of genetic diversity (H, π, and θ), divergence (d_{xy}), and differentiation (F_{ST}) at intergenic (I) and fourfold degenerate (4D) sites between *I. feisthamelii* and *I. podalirius*. Estimates for 4D sites are taken from (Ebdon et al., 2021).

	H_{I}	H_{4D}	π_{I}	θ_{I}	$d_{\mathrm{xy,I}}$	$d_{\mathrm{xy,4D}}$	$F_{\mathrm{ST,I}}$	$F_{\mathrm{ST,4D}}$
I. feisthamelii	0.00676	0.00794	0.00682	0.00692	0.0244	0.0275	0.594	0.575
I. podalirius	0.00585	0.00521	0.00652	0.00659				

modelling the shared genealogical history of closely linked variants in the composite likelihood framework implemented in `gIMble`. To maximise the density of neutrally evolving sites we follow Laetsch et al. (2023) and restrict this analysis to intergenic sequence which have similar per site diversity and divergence to fourfold degenerate (4D) sites in coding regions (Table 1). After applying coverage based filters (see Methods), our analyses include 39% of the genome ($\approx$ 160 out of 408 Mb).

We fit a series of demographic models to the blockwise site-frequency spectrum (bSFS) of the whole genome: a model of strict divergence (DIV) and an IM model with migration in either direction with three N_{e} parameters ($IM_{3,\rightarrow\mathrm{pod}}$ and $IM_{3,\rightarrow\mathrm{fei}}$). Out of these three scenarios (Table 2), the best fitting history is an IM_3 model with unidirectional gene flow (forwards in time) from *I. feisthamelii* into *I. podalirius* ($IM_{3,\rightarrow\mathrm{pod}}$). Since an IM model will always fit at least as well as the (nested) DIV model, we compared the observed improvement in model fit ($\ln CL$) relative to the null distribution of $\ln CL$ which we obtained by simulating 100 data sets under the best fitting DIV history and fitting IM models (see methods). This parametric bootstrap confirms that the $IM_{3,\rightarrow\mathrm{pod}}$ model does indeed fit significantly better than a DIV_3 history (Fig S1).

Under the background/global IM model, we infer a split time (T) 2,180,000 generations ago (Fig 2, Table 2) and N_{e} estimates of 483,000, 377,000 and 1,140,000 for *I. feisthamelii* and *I. podalirius* and the ancestral population, respectively. This split time is close to previous estimates for the species pair (Ebdon et al., 2021). The long-term genome-wide rate of gene flow m_{e} from *I. feisthamelii* into *I. podalirius* is 4.73 $\times 10^{-8}$ which corresponds to $M/2 = 2N_{\mathrm{e}}m_{\mathrm{e}} = 0.046$ migrants per generation.

Extensive genome-wide reproductive isolation between *I. feisthamelii* and *I. podalirius*

We infer the effective migration rate m_e along the genome in sliding windows. For each window, we estimate parameters under the best fitting $IM_{3,\rightarrow\mathrm{pod}}$ history using a pre-computed grid. Note that whilst the split time T is fixed globally, the remaining four parameters (N_{e} for each population and

m_e) are estimated locally, i.e. per window. The estimates of local N_e are approximately normally distributed (Fig S2). In contrast, local m_e estimates have a strongly leptokurtic distribution with a peak at $m_e = 0$ and a long tail up to the maximum value in the grid (Fig S2). Note that the large number of windows in the largest m_e bin reflects the fact that our grid of m_e estimates necessarily truncates the m_e distribution, but does not affect our analyses of barriers.

Following Laetsch et al. (2023) we label windows as barriers to gene flow if a DIV history ($m_e = 0$) has greater marginal support than an IM history assuming the best fitting genome-wide value of m_e (Table 2) and this difference in marginal support is supported by a parametric bootstrap (see methods), i.e. $\Delta_{B,0} > 0$. Applying this strictest possible barrier definition, we find that barriers to gene flow are widespread in the *Iphiclides* genome, making up 20% of windows across all chromosomes. Combining overlapping barrier windows, we define 555 barrier regions across all autosomes which cover 33% of the genome ($\approx$ 143Mb). The average length of barrier regions is $\approx$ 257 kb (median $\approx$ 200 kb) with a maximum of 1.4 Mb.

The genomic correlates of long-term barrier regions

Assuming that the causal loci underlying barriers are in or near genes, we predict an enrichment of long-term barriers regions for coding sequence. This pattern has been observed in *Heliconius melpomene* and *H. cydno* (Laetsch et al., 2023) as well as scans for pairwise incompatibilities in natural hybrid populations of sword tail fish (Schumer et al., 2018). Contrary to this expectation, we find that both the density of coding sequence (CDS) and repeats are reduced in barrier regions (Fig S3, see discussion). Given that our windows are both overlapping and genetic variation is autocorrelated along the genome (due to LD and various other sources of autocorrelation) standard statistical methods that assume independence are inappropriate for assessing the significance of differences between barrier and non-barrier windows and would lead to vastly overconfident conclusions. Instead, we use a circular data bootstrap approach to quantifying the statistical support for correlates of barriers throughout. This is inspired by a similar circular resampling scheme used by Yassin et al. (2016) and Nouhaud et al. (2022) who resampled by circularising the genome and sampling datasets with fixed offsets. We modify this procedure to sample with random offsets and circularising each chromosome (rather than the whole genome). This allows us to obtain null distributions for any genomic measure (e.g. CDS density) for a random sets of genomic windows that have the same distribution between and distances/clustering within chromosomes as the set of barrier windows inferred by `gIMble`. Applying this data bootstrap confirms that both CDS

and repeat density are indeed significantly reduced in long-term barriers compared to non-barrier windows (Fig S3).

Models of local adaptation under migration selection balance predict a concentration of barriers in regions of low recombination and a positive correlation between m_e and recombination (Barton and Hewitt, 1985). While we lack direct estimates of recombination for *Iphiclides* we can use chromosome location as an indirect proxy for recombination over two scales. First, given the restriction of a single cross-over per meiosis (Mather, 1938), chromosome length is inversely related to recombination rate (Stapley et al., 2017; Martin et al., 2019; Näsvall et al., 2023). Second, an ubiquitous feature of meiosis in Lepidoptera is that – despite the lack of centromeres – recombination is reduced in the centre of chromosomes. Indeed, heterozygosity is strongly correlated with chromosome length in both *I. podalirius* (Pearson's ρ = -0.827, p = 3.18e-9) and *I. feisthamelii* (Pearson's ρ = -0.856, p = 3.19e-9) and is lower towards the center of chromosomes (Figs. S4C, S5). We therefore expect both long chromosomes and chromosome centres to be enriched for barriers to gene flow. In line with these predictions we find that barriers are correlated with recombination rate variation between and within chromosomes. First, both the proportion of barrier sequence (Pearson's ρ = 0.43, p = 0.0241, Fig S4A) and the average m_e (Pearson's ρ = -0.55, p = 0.00195) are correlated with chromosome length. Second, we observe that, on average, barrier regions are closer to the centre of chromosomes than non-barrier regions (circular bootstrap, p = 0.001 Fig S4C). The number of barrier regions varies widely between chromosomes: e.g. chromosomes 29 and 31 harbour no and one barrier region, respectively. In contrast, chromosomes 19 and 17 have 53 (29.3% of windows) and 49 (29.5% of windows) barrier regions, respectively (Fig S6).

Genome polarisation reveals complex hybrids

Chromosome-painting of individual genomes via diagnostic markers provides a direct way to visualize the mosaic ancestry of HZ samples (Meier et al., 2021; Iasi et al., 2024; Saarman et al., 2019). While many studies have relied on assigning hybrid genotypes based on a reference panel which is assumed to reflect 'pure' ancestry, this assumption is both unnecessary and biases inference against introgression (Gompert et al., 2017). We labeled the ancestry of alleles at all non-singleton SNPs with respect to the focal (i.e. between species) barrier using the EM algorithm implemented in `diem` (Baird et al., 2023). This approach requires no *a priori* defined sets of reference individuals or candidate variants and assigns genotypes of 0/0, 1/1 or 0/1 at each variant position which correspond to homozygous for each species or heterozygous by source respectively. Note that although

all samples were included in the polarisation we focus our analysis of recent introgression on the "HZ set" of six individuals (Fig 1 B).

Genome polarisation shows that the HZ individuals (Fig 1B) have an alternating pattern of *podalirius*—*feisthamelii* ancestry along all autosomes (Fig 3) which can only be generated by hybridisation after divergence. We find substantial heterogeneity in the degree of hybridisation, as quantified by the hybrid index (HI) which is defined as the average across genotype assignments in an individual, both between individuals and chromosomes (Fig 4). The two most intermediate HZ samples, IF_1325 ($HI = 0.712$) and IF_1322 ($HI = 0.420$), show large stretches of all three possible ancestries, a pattern that reflects a complex history of hybridisation: the expected HI of a simple n-th generation backcross hybrid is $(1/2)^n$ with homozygous tracts for one species only. While we expect substantial variation around this expectation, successive generations of simple backcrosses move the expected HI towards the parental values of 0 or 1 along the sides of the ternary plot of HI against H. In other words, interspecific H (the proportion of genotypes with an allele from each side of the barrier) remains maximal. Thus, the relationship between the HI and interspecific H shows that samples 1325 and 1330 are complex backcrosses (i.e. their ancestry is incompatible with a successive backcrosses with pure parental individuals), and suggests that in both cases introgression is towards *I. podalirius* (Fig 4A). Interestingly, all HZ samples except 1322 show a deficit in interspecific heterozygosity relative to Hardy Weinberg equilibrium (HWE) (Fig 4) which is the expectation for genotype frequencies under a null model *senu* Barton that assumes per locality, per locus HWE and a uniform admixture process along the genome. Thus the deficit in heterozygosity suggests local substructure/inbreeding in the HZ and/or selection against heterozygous (by source) ancestry which may be driven by partially dominant incompatibilities. Strikingly, we find that the six HZ individuals (which includes two male samples) only exhibit one Z chromosome of mixed ancestry (1325, a female), which suggests that the Z is a substantially greater barrier than autosomes of equivalent length, as predicted by numerous theoretical models (Charlesworth et al., 1987; Mank et al., 2009; Bachtrog et al., 2019; Turelli and Orr, 1995).

Long-term barriers to gene flow are associated with regions of low hybridity

Setting up a comparison between barriers to long-term introgression and gene flow across the *Iphiclides* HZ requires a measure of barrier strength that extracts information contained in the small sample of HZ individuals. Classic theory for hybrid zone barriers is couched in terms of cline parameters which cannot be meaningfully estimated from a sample of six individuals. Nevertheless,

it is clear that chromosome paintings even for a small sample of individuals contain a wealth of information about recent introgression. For example, assuming that our sample of six HZ individuals is centered, a genomic region without any gene flow (i.e. a complete short term barrier region) is expected to be painted entirely homozygous for *I. podalirius* and *I. feisthamelii* ancestry for three individuals on either side of the centre (clines would be maximally narrow, stepped, and steep). To capture the information about the local strength of barriers to local gene flow contained in a small set of polarized hybrid genomes, we estimated $\bar{D}$ (Barton and Gale, 1993), the multi-site mean pairwise LD, in windows defined in the `gIMble` analysis. This is numerically equivalent to the variance in HI and captures the strong LD seen along stretches of co-introgressing variation: when minimal for polarised data ($D = 0$), states of sites are uncorrelated, and when maximal ($D = 0.25$), each sample reflects pure ancestry.

We find that — at the scale of `gIMble` windows ($\approx$ 100 kb) — $\bar{D}$ is negatively correlated with $m_{\mathrm{e,i}}$ (Pearson's ρ = -0.57, p = 0.0). To test whether short-term barrier strength (as measured by $\bar{D}$) is greater within long-term barrier windows than expected by chance, we conducted two different circularised bootstrap schemes to obtain null distributions for $\bar{D}$: either circularising each chromosomes (accounting for differences in the number of barriers between chromosomes) or circularising the whole genome (not accounting for chromosome effects). We find that the mean $\bar{D}$ for barrier windows is significantly greater than either of these resampled distributions (circular bootstrap, $p < 0.001$, Fig 5B). This suggests ongoing selection against hybrid ancestry within the HZ at long-term barrier loci (Fig 5A). While the upward shift in the resampled distributions accounting for chromosome of origin suggests that between-chromosome variation in recombination rate does contribute a small effect, the overlap between long and short term barriers cannot be explained by the fact that both $\bar{D}$ (Pearson's ρ = 0.74, p = 4.84e-06) and barrier density are correlated with chromosome length (Fig S4A & B).

While $\bar{D}$ is an obvious measure of short-term barrier strength that is straightforward to compute from a set of `diem` polarized genomes, we also considered two alternative measures of short-term barrier strength: i) the local density of strongly diagnostic ($DI > -14$) sites and ii) the total number of unique ancestry junctions in windows. Firstly, we expect that sites which are more strongly diagnostic of population differentiation will be in greater LD with regions of low gene flow across the HZ by definition. We find that sites with high diagnostic indices are more densely populated within barrier windows relative to a null resampled distribution (circular bootstrap, $p < 0.001$, Fig 5C & D). Secondly, the number of unique ancestry junctions per window should negatively correlate with barrier strength, as selection against admixture will limit the decay of

admixed block sizes generated by successive introgression. Thus, a given barrier region should be populated by fewer and larger blocks of co-ancestry, and necessarily, fewer junctions than migrating regions. Indeed, we find that barrier regions contain almost half the number of ancestry junctions than expected by chance (circular bootstrap, $p < 0.001$, Fig 5E & F). Our finding that long-term barriers show reduced introgression across the HZ as measured by the three HZ barrier-strength metrics were not driven by any one HZ sample and were robust to the exclusion of individual HZ samples (circular bootstrap, $p < 0.001$ in all six instances for each metric).

Modelling the history of introgressed blocks in complex hybrids

We have so far interrogated the data for the six HZ individuals in terms of the variation in the strength of short term barriers, both between and within chromosomes. However, theoretical models of multilocus barriers consider the aggregate effects of many loci under selection. This creates a genome-wide barrier that (assuming a model of uniformly distributed selection targets) can be captured by the ratio between the selection pressure and the recombination rate, a.k.a. the coupling coefficient $\theta = S/R$ (Barton, 1983; Barton and Hewitt, 1985; Baird, 1995). Thus an obvious question is: what strength of multilocus selection is the mosaic ancestry of the six HZ individuals compatible with? To address this, we considered the length distribution of introgression tracts. If we make the simplifying assumption that introgression across the HZ into either species started at time T, occurs at a constant rate m, and only involves backcrosses (i.e. the recipient population is infinitely large), the lengths of admixture tracts depend only on the coupling coefficient θ (Barton, 1983; Barton and Hewitt, 1985; Baird, 1995). More precisely, the equilibrium solution for the gradient of the admixture tract length distribution on a log-log scale is $-\frac{3+\theta}{1+\theta}$ (see Fig 6, Appendix 1). Thus, to learn about the direction and dynamics of recent gene flow across the HZ, we fit the distribution of admixture tract length of colinear introgressed ancestry to the analytic expectation under this model (Baird, 1995). In the absence of a recombination map, we measured the length of admixture tracts (x) relative to chromosome length, i.e. we assumed that each autosome has a map length of 25 cM, which corresponds to an average of one cross-over event per male meiosis (female butterflies are achiasmatic). To avoid block lengths being fragmented by rare errors and gene conversion events, we kernel smoothed `diem` labeling along chromosomes at a scale of $10^{-4}\times$ chromosome length, which corresponds to >1kb for most autosomes.

Considering long tracts ($l > 0.04$), neutrality provides a good fit for the distribution of tracts of *I. feisthamelii* ancestry in *I. podalirius* (i.e. a gradient of -3). In contrast, the size distribution

Table 2 – Maximum composite likelihood parameters for three demographic models of species divergence. We use the $IM_{3,\rightarrow\text{pod}}$ model for barrier inference. $\Delta \ln CL$ is relative to the best supported model (bold).

model	N_{fei}	N_{pod}	N_{anc}	T	m	$\Delta \ln CL$
DIV	459,000	416,000	1,240,000	1,810,000	-	-389,374
$\mathbf{IM_{3,\rightarrow\text{pod}}}$	**483,000**	**377,000**	**1,150,000**	**2,180,000**	**4.73E-08**	**0**
$IM_{3,\rightarrow\text{fei}}$	438,000	429,000	1,190,000	2,020,000	2.80E-08	-238,736

of *I. podalirius* admixture tracts in *I. feisthamelii* is best explained by $\theta = 0.44$ (Fig 6). This asymmetry mirrors the asymmetry of long-term gene flow under the IM history inferred by `gIMble` and suggests that gene flow has been stable for much of the last 150 - 275 generations (75 - 140 years). In contrast, over the same timescale *I. podalirius* admixture into *I. feisthamelii* has been strongly selected against. Interestingly, we find that the admixture tract length distribution in neither direction involves a simple asymptote for short tracts as predicted for a secondary contact initiated at time T with constant m. This may be due to several factors: first, gene flow in the more distant past may have been genuinely lower, which — given the dependence of *Iphiclides* on orchards and other anthropogenic habitats — may reflect changes in landscape use. Secondly, our simplistic measure of x as a proportion of chromosome length is inadequate for short blocks; given that the recombination is known to vary substantially along butterfly chromosomes (Martin et al., 2019). Thirdly, our model is unrealistically simplistic in that it ignores space: it assumes introgression into an infinitely large panmictic population. In a spatially continuous population we expect shorter tracts with increasing distance from the HZ which is indeed what we observe in *Iphiclides*. Fourthly, violating our infinite population size assumption, hybrids in finite populations can interact, producing complex admixture tracts. This may inflate the distribution of small tracts in both admixture directions and explain the asymmetric deviation from expectation we see between fits. Finally, it is also plausible that the polygenic model of barrier architecture assumed by Baird (1995) breaks down over short scales, because it does not include the possibility that increasingly short blocks may have increasingly variable fitness effects (including the possibility of adaptive introgression).

Discussion

Much of the recent research on the genomics of speciation has focused either on fitting demographic models to estimate migration over timescales of N_{e} generations (Excoffier et al., 2013; Aeschbacher et al., 2017; Mondal et al., 2019; Fraïsse et al., 2021) or on investigating barriers to recent introgres-

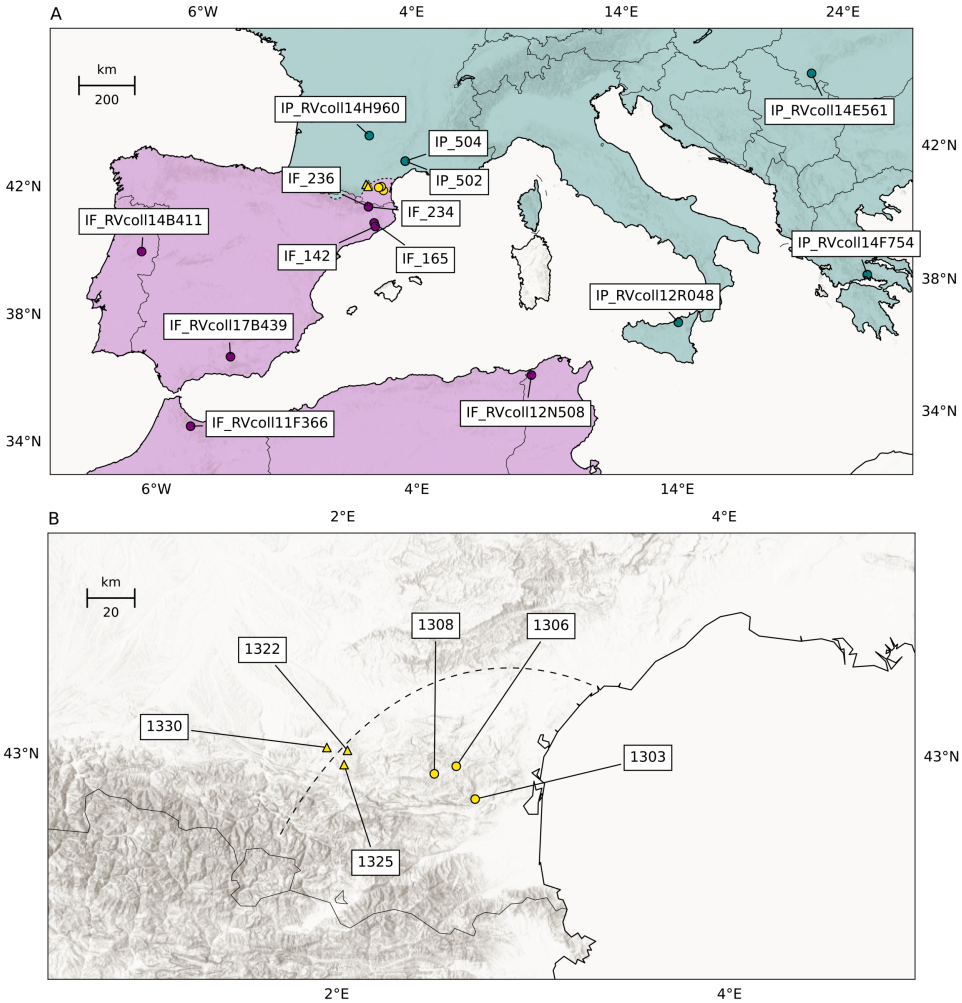

Figure 1 – (A) Sampling locations and ranges of *I. feisthamelii* (purple) and *I. podalirius* (teal) butterflies. The samples collected from the hybrid zone (HZ) are shown in yellow. (B) Sampling locations of butterflies from the *Iphiclides* HZ. The dashed line represents the approximate HZ center, based on samples collected by Lafranchis et al. (2015). The circular samples resemble *I. feisthamelii* (HI < 0.1), the triangular samples are intermediate hybrids (HI > 0.1).

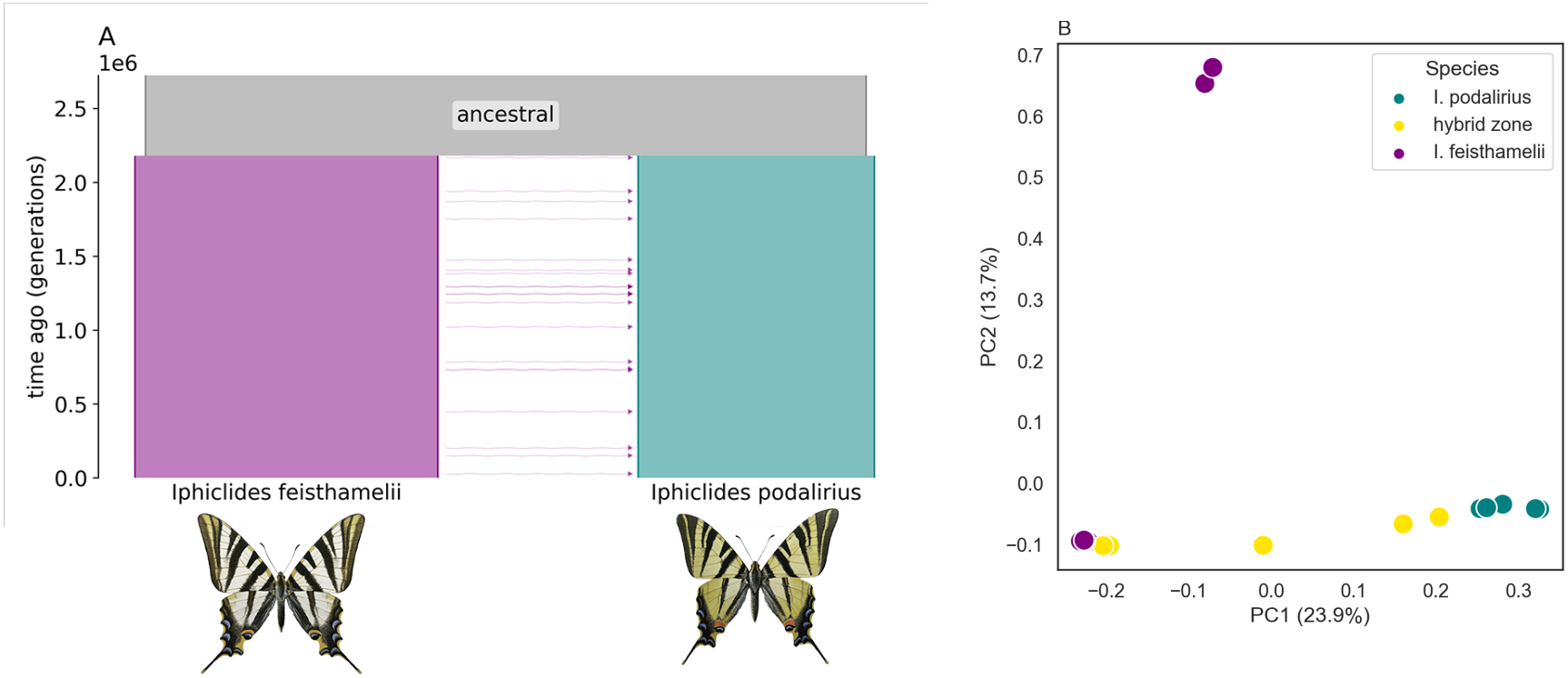

Figure 2 – (A) The background demographic history of species divergence and gene flow, the height and width of populations, is relative to the maximum likelihood estimates under the $IM_{2,\rightarrow pod}$ model (Table 2). This figure was generated using *demes* (Gower et al., 2022). (B) PCA of *Iphiclides* sampled across Europe; *I. feisthamelii* and *I. podalirius* samples are shown in purple and teal respectively. Samples from the HZ are shown in yellow: PC1 captures differences between the two taxa, PC2 geographic structure, particularly the separation between North African and European *I. feisthamelii*.

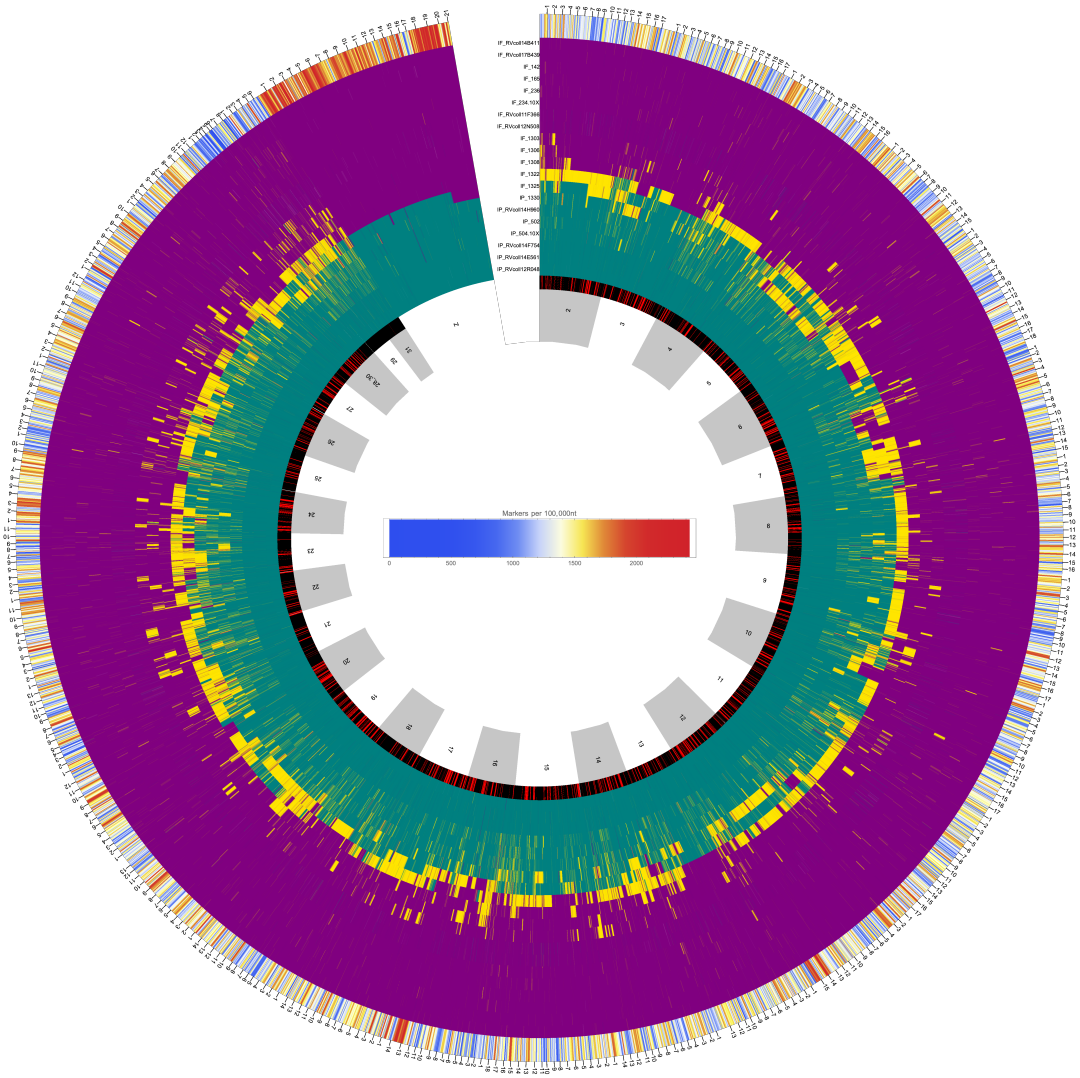

Figure 3 – Circular representation of the location of barriers identified using *gIMble* and the polarity of diagnostic markers for each sample across linkage groups. The inner ring shows the location of each chromosome in alternating grey and white. Moving outwards, the next ring indicates the location of barriers to gene flow (in red) and non-barrier/migrating regions (in black). The remaining rings show the genotype of each sample at each diagnostic marker. Teal bars are diagnostic of *I. podalirius*, purple bars are diagnostic of *I. feisthamelii*, and yellow bars are heterozygous for markers diagnostic of each species. The outermost ring shows the density of high DI sites. The location of each megabase of sequence for each chromosome is indicated on the outside of the circle.

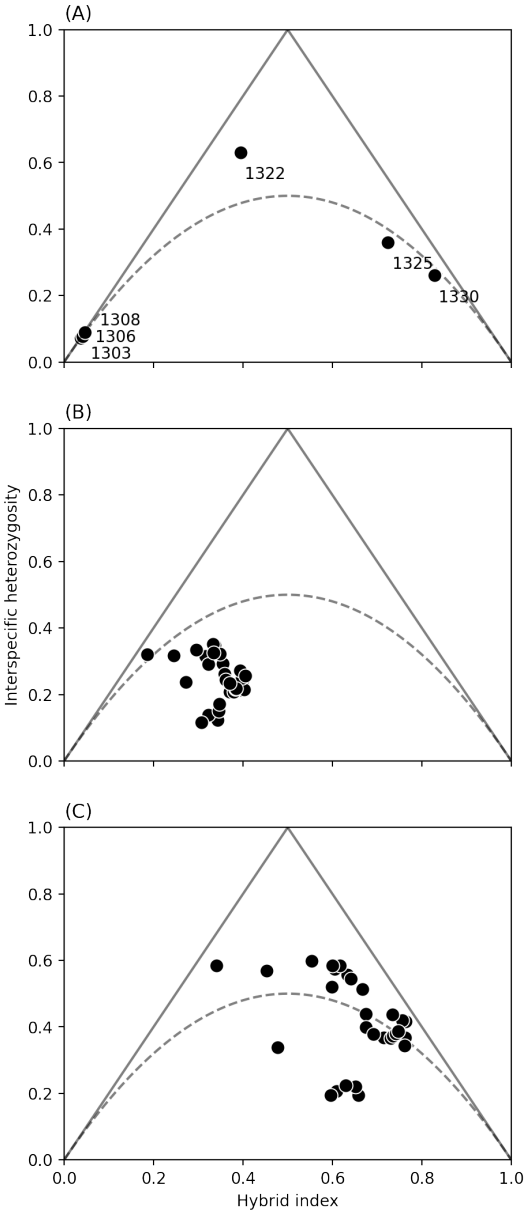

Figure 4 – Hybrid index (HI) versus interspecific heterozygosity (H) for samples collected from the *Iphiclides* hybrid zone (HZ) (A) Mean values for each HZ sample. (B) Mean values for each chromosome including all samples from the HZ. (C) Mean values for each chromosome excluding the three *I. feisthamelii*-like samples (1303, 1306 and 1308, $HI \approx 0$). The dashed line indicates the expectation under Hardy-Weinberg equilibrium.

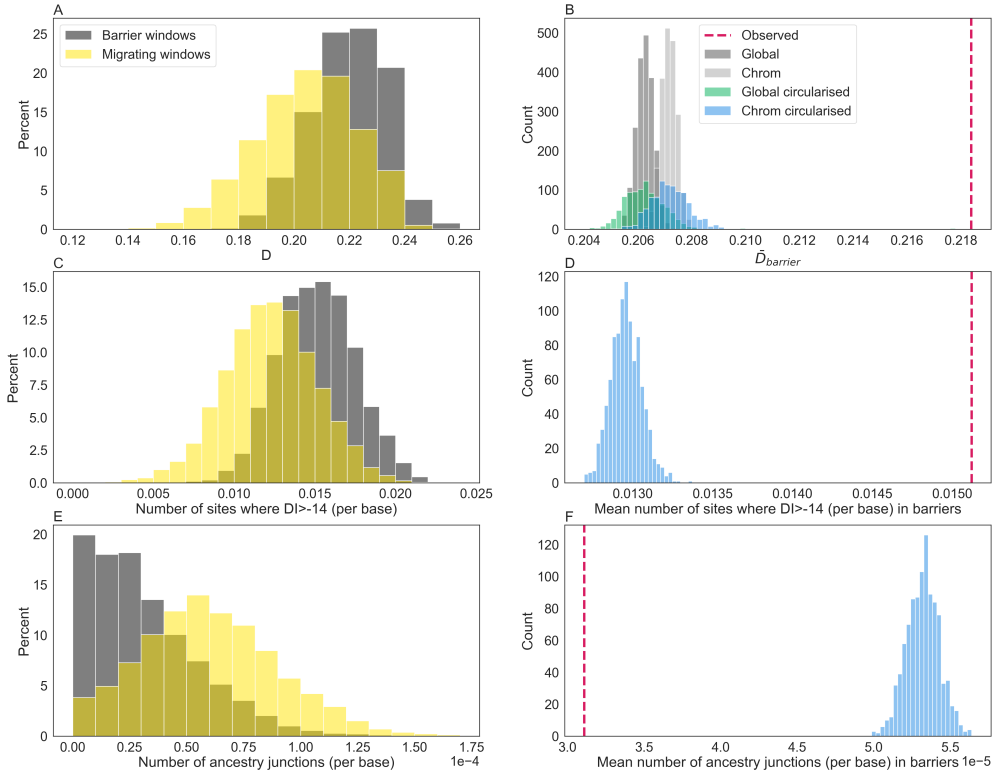

Figure 5 – The distributions of $\bar{D}$, the number of strongly diagnostic sites, and the number of unique ancestry junctions (A/C/E) across *gIMble* barrier windows (grey) and non-barrier/migrating windows (yellow) and their corresponding bootstrap results (B/D/F). The latter two metrics have been corrected for window span. Both $\bar{D}$ calculated per window (A & B, circular bootstrap, $p < 0.001$) and the number of highly diagnostic markers (C & D, circular bootstrap, $p < 0.001$) is greater within long-term barriers than in non-barrier windows. The number of unique ancestry junctions is lower within long-term barriers than in non-barrier windows (E & F, circular bootstrap, $p < 0.001$). Null distributions of $\bar{D}$ were generated using four different resampling schemes (B). In each instance, random values of $\bar{D}$ were drawn without replacement from the empirical distribution of window-wise $\bar{D}$ to generate datasets corresponding to the number of barrier windows. We repeat each resampling 1,000 times and compare the distribution of mean $\bar{D}$ to the observed value. Firstly, we sample datasets from the entire genome with (green) and without (black) circularising (see methods). Secondly, we resample per-chromosome accounting for differences in the number of outliers between chromosomes, also with (blue) and without (grey) circularising. We only show the most conservative test - the circular bootstrap accounting for chromosome-of-origin - for the number of strongly diagnostic sites (D) and the number of junctions (E).

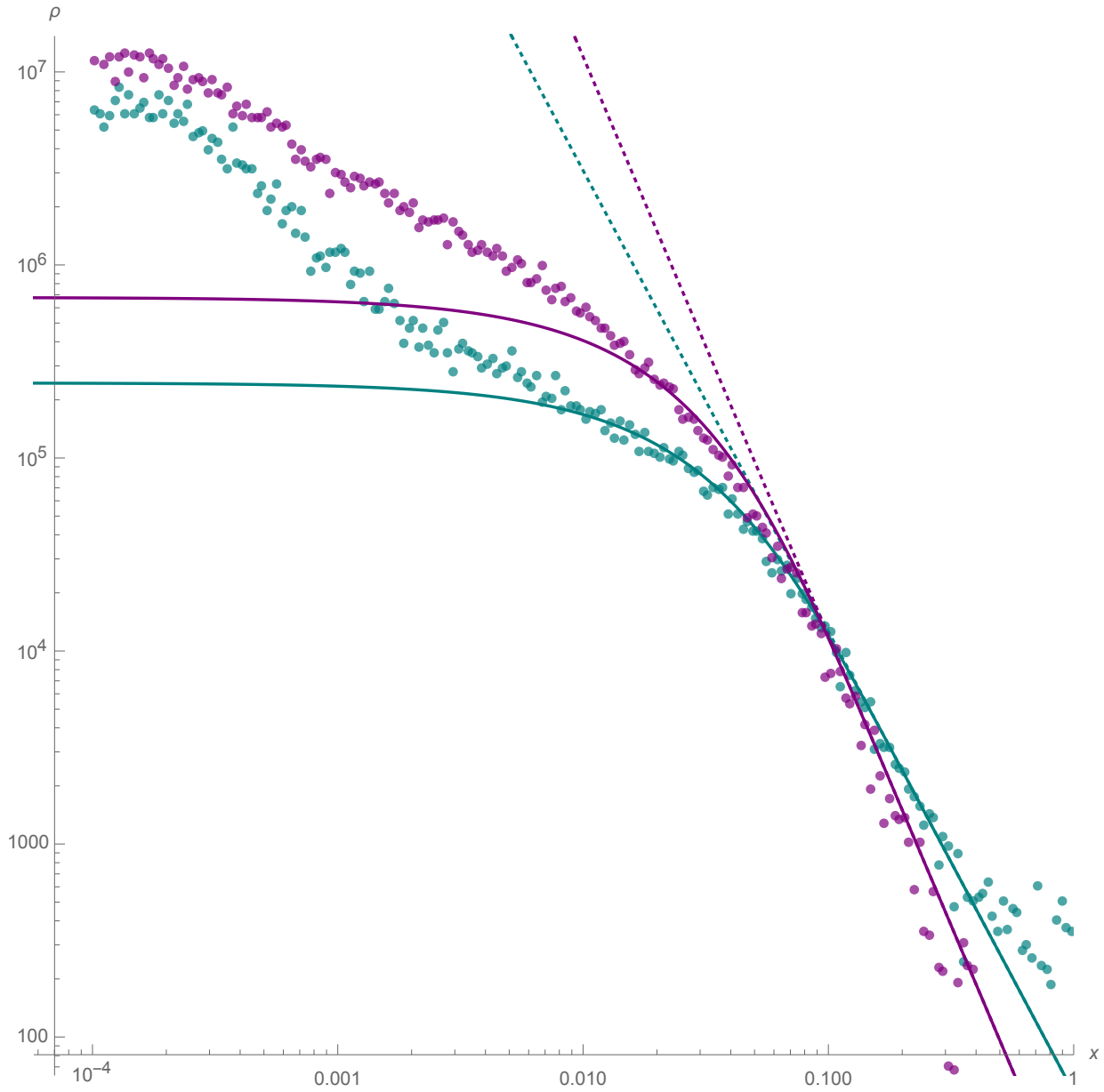

Figure 6 – Distribution of sizes of (purple points) *I. feisthamelii* tracts introgressing into *I. podalirius*, and (teal points) *I. podalirius* tracts into *I. feisthamelii*, on a log-log scale. Note, as most introgression is heterozygous, the introgressing tracts largely correspond to the yellow tracts in Figure 3. These are compared to theoretical predictions (solid lines) for exchange between two infinite demes (Appendix A-5). Introgression into *I. podalirius* is plotted for [M, S, R, T = 15, 0.11, 0.25, 150]. Introgression into *I. feisthamelii* is plotted for [M, S, R, T = 1.5, 0.0, 0.25, 275]. The difference in gradients on the right indicates stronger coupling (S/R) of the *I. podalirius* background despite more migrants M per generation. The distribution of small blocks towards the left does not match theory (see Results), making the time-since-contact estimates T lower bounds only.

sion (10s or 100s of generations) in studies of HZs (e.g. Buggs, 2007; Teeter et al., 2008; Macholán et al., 2011; Hagberg et al., 2022), natural hybrid populations (Schumer et al., 2018) and laboratory crosses studies (e.g. Turner and Harr, 2014; Poikela et al., 2022). However, there are surprisingly few attempts to understand how barriers to gene flow on these two timescales are related. Here we have fitted explicit demographic models of speciation to infer the heterogeneity in long-term effective migration between two sister species of *Iphiclides* butterflies. We intersect this inference with signals of recent, heterogenous introgression across a HZ estimated from a small set of HZ individuals using genome polarisation.

Evidence for both long-term and recent gene flow between the scarce swallowtails

We find that the long-term demographic history of *I. podalirius* and *I. feisthamelii* is well approximated by an IM model with a low rate of unidirectional migration ($M = 2N_{\mathrm{e}}m = 0.046$) from *I. feisthamelii* into *I. podalirius*. Thus our analysis adds to the growing number of young species pairs for which a signal of long-term and ongoing migration has been identified, including great apes (Mailund et al., 2012), butterflies (Martin et al., 2013; Capblancq et al., 2019; Mackintosh et al., 2023), mollusks (Hirase et al., 2021), angiosperms (Papadopulos et al., 2011), birds (Reifová et al., 2016), *Drosophila* (Garrigan et al., 2012), and many more.

However, we note that the global effective migration rate (m_e) we infer in *Iphiclides* is considerably lower than estimates obtained for sister species pairs of *Heliconius* (Laetsch et al., 2023) and *Brenthis* (Mackintosh et al., 2023) butterflies, both of which are of comparable age (Fig S7). Although this low background level of genome-wide migration reduces the power to identify individual barrier regions, it still allows quantification of the variation of m_e and its correlates along the genome. Furthermore, we find evidence for ongoing introgression between the two *Iphiclides* species across a HZ in the form of complex hybrids. Relating the distribution of admixture tract lengths to analytic expectations under a model of secondary contact (Baird, 1995) suggests that recent gene flow into *I. podalirius* is neutral, while gene flow into *I. feisthamelii* is strongly selected against. This asymmetry is concordant with the inferred direction of long-term gene flow. It is also consistent with genetic load arguments, which predict stronger selection against admixture tracts derived from the taxon with lower N_e (Harris and Nielsen, 2016), i.e. *I. podalirius* in this case.

More generally, it is encouraging how much information about both recent and long-term introgression is contained in a small sample of individual genomes. Given that most species pairs do not have HZs, such long-term barrier inference is the only genomic information available about

their speciation history. Even when HZs exist, they may not be amenable to clinal analyses due to sampling constraints as is the case for *Iphiclides*. However, our analyses demonstrate that the genome-wide barrier which is described by the coupling coefficient and the recent history of gene flow can be estimated from a handful of HZ individuals. It is perhaps surprising how well the admixture tract lengths we observe in *Iphiclides* fit analytic expectations under the simplest possible model of secondary contact which assumes panmixia, infinite population size and weak selection (Baird, 1995). The fact that the observed length distribution deviates from this expectation for short tracts suggests that small samples of hybrid genomes contain additional information about admixture. In particular, it would be interesting to fit models of more realistic barrier architectures that assumes a large but finite number of loci. Furthermore, classic theory on Fisher junctions for HZs only considers the decay of admixture tracts due to crossover events (Barton, 1983). However, the internal decay of admixture tracts due to gene conversion events has so far been ignored and overlays the effects of an additional clock.

The ability to estimate the genomic distribution of block sizes (Fig 6) and relate it to theory (Baird, 1995) developed long before genomic data were available is thrilling. The distribution of large blocks is expected to reach equilibrium quickly, and appears log-log linear suggesting relatively strong coupling of 0.44 at least in one direction. Neither direction reaches the 'tipping point' coupling of $S/R = 1$ (Barton, 1983), where multilocus clines 'congeal', however that sharp threshold at equilibrium is misleading. Because small blocks equilibrate very slowly, it would take longer than an interglacial period for a sharp distinction in secondary contact outcome to be perceivable (Baird, 1995) (Fig 2).

Long and short-term barriers to gene flow

The fact that barriers, inferred over these two time-scales of evolution, overlap shows that a significant subset of barriers is persistent and acts at very different points of the speciation continuum. This suggests that regions of the genome that maintain reproductive isolation between species in the long-term are also relevant in early species divergence. Indeed, in *Heliconius* butterflies it has been shown that the same wing pattern genes maintain species differences both across HZs (Nadeau et al., 2014) and in deep time (Laetsch et al., 2023). However, in contrast the congruence in barrier landscapes across timescales we find in *Iphiclides* is not restricted to a small number of large effect genes, but rather a genome-wide phenomenon, suggesting a polygenic barrier architecture.

We would argue that this internal comparison of long-term barrier landscape with short-term

barriers is a more promising avenue for testing of models of speciation than comparisons/contrasts of species at different stages, which invariably differ in speciation history and barrier architecture (Johnson and Miyanishi, 2008; Mérot et al., 2017; Stankowski and Ravinet, 2021). Thus, an important direction for future work is to develop quantitative predictions for the temporal change in barrier landscapes. Under an allopatric null model, which may apply to *Iphiclides* during glacial periods, pairwise intrinsic incompatibilities are assumed to accumulate at random positions in the genome and genome-wide coupling is expected to increase quadratically with time (Orr, 1995). Under this model, we expect a limited amount of temporal barrier overlap which arises from the fact that barrier loci that establish early have a greater effect on long-term m_e than later barriers. In contrast, verbal models of 'divergence hitchhiking' assume that early barriers expand locally (Wu, 2001; Nosil, 2008) and so may predict a greater degree of temporal overlap. While theoretical models show that locally expanding barriers are possible — given sufficiently strong selection and linkage (Otto, 2019) — there is so far not much empirical evidence that locally expanding 'islands of speciation' are a common feature of speciation.

The architecture of barrier loci

We found substantial variation both in the size of barrier regions and in the proportion of barrier sequence per chromosome. Specifically, barriers to gene flow aggregate on large chromosomes and towards chromosome centres. Both are regions of the genome for which recombination rates are reduced, as we expect from barrier loci that individually confer small effects. This is consistent with previous research on *Heliconius* butterflies, which demonstrated that barriers to introgression are concentrated in regions of low recombination (Martin et al., 2019; Laetsch et al., 2023), and supports a polygenic barrier architecture. Such architecture was originally proposed as a null model of reproductive isolation (Barton and Charlesworth, 1984) and evidence of polygenic barriers to gene flow has accumulated across a range of taxa (Szymura and Barton, 1986; Macholán et al., 2007; Turner and Harr, 2014; Morán and Fontdevila, 2014). Thus, it appears on a broad scale that the architecture of reproductive isolation between *Iphiclides* species is strongly linked to recombination rate heterogeneity.

We investigated whether barrier regions are associated with particular genomic features and failed to find enrichment of repetitive elements or more surprisingly, coding sequence, as one might expect if reproductive isolation is driven by selection on genes. Our circular resampling procedure controls for differences in gene and repeat density between chromosomes, so it is clear that the

reduced gene density for barrier regions (circular bootstrap, $p < 0.001$, Fig S3) is not simply a consequence of the negative correlation between gene density and chromosome length and the fact that barrier density is higher for long chromosomes. However, it may be that the effect of intra-chromosomal variation in recombination rate vastly outweighs the impact of coding sequence density.

Limitations

To infer barriers to gene flow conservatively, we use the strictest possible threshold ($m_{\mathrm{e,i}} = 0$) and quantified the false positive rate (FPR) in a parametric bootstrap (see methods). Whilst this potentially excludes actual barriers with $m_{\mathrm{e,i}} > 0$ at putatively neutral flanking regions — which are the basis/input of our inference — this minimises the FPR.

Numerous factors may contribute to biases in our results (see Ravinet et al. (2017), and Laetsch et al. (2023) for `gIMble` limitations). Given that a directly estimated recombination map does not yet exist for *Iphiclides*, we cannot directly quantify the degree to which recombination rate heterogeneity contributes to migration rate variation nor account for the fact that uncertainty in estimates of both short and long-term barriers depends on the local recombination rate.

There may be scope to improve the power to detect weak gene flow through modelling more detailed demographic scenarios. Firstly, whilst it is very likely that the *Iphiclides* pair has undergone repeated rounds of separation and gene flow, we have fit a much simpler model that assumes a single continuous rate of migration. Secondly, we have modelled gene flow as unidirectional and inferred the most likely direction by comparing models. In reality, gene flow between these species may be bidirectional but asymmetric, as estimates in other systems suggest (Yan et al., 2016; Ngeve et al., 2017; Banker et al., 2022). Expanding the `gIMble` framework to include isolation with initial migration (IIM) and bi-directional gene flow may improve our power to model the build-up of genomic barriers (Wilkinson-Herbots, 2008; Laetsch et al., 2023).

The `diem` genome polarisation algorithm is designed to work with even small amounts of low quality data. There should therefore be few power limitations working with high quality genome scale data, and indeed estimates of hybrid indices, interspecific heterozygosity, and visualisation of admixture have high precision (Baird et al., 2023). Estimating admixture tract size distributions requires a further level of precision however: a single ancestry state error in a long block will on average halve its estimated length, error due to a miscalled variant would affect one tract, but error due to a mispolarised site could affect many. To avoid such error driven tract fragmentation, we filter

polarised sites for high diagnostic index — strongly correlated with the support for correct polarity — and introduce an arbitrarily chosen scale of kernel smoothing of state along chromosomes. This has an advantage over HMM approaches in that it has no starting point chirality, but the disadvantage that it censors true small tract signal with some distribution of false negatives. This likely contributes to the departure of small tract observations from simple expectations (Fig 6).

Finally, one of the most striking results of our analysis of HZ is the scarcity of introgressed ancestry tracts on the Z chromosome (Fig 3). While we have not quantified the density of gIMble barriers on the Z (because such an analysis would be limited to male samples), it will be fascinating to investigate the long term evolution of Z linked barriers in *Iphiclides* in the future.

Conclusion

We have demonstrated an association between long-term and short-term reproductive isolation in a species pair of swallowtail butterflies. Despite being several million generations old, gene flow persists between these species and is currently concentrated at a HZ. The considerable number, varying size, and location of barrier regions suggest that the genomic architecture of speciation is polygenic, or multilocus *sensu* Barton (1983). We find that variation in m_e correlates with proxies of recombination rate variation both between and within chromosomes and so is likely shaped by recombination rate heterogeneity, a pattern previously observed in *Heliconius* butterflies (Martin et al., 2019; Laetsch et al., 2023). However, in the absence of a directly estimated recombination map, it is impossible to know to what extent the overlap between long and short-term barriers reflects a shared/stable recombination landscape rather than shared selective targets. Unlike genomic cline methods (Gompert and Buerkle, 2012), our approach maximises information contained in small samples about barriers to gene flow over different time scales. This paves the way for future quantitative analyses of the temporal evolution of the genomic landscape of species barriers. While most speciation processes are far too slow to observe directly, genomic variation clearly contains information about the interplay of forces acting at different stages of the speciation continuum.

Methods

Sampling and sequencing

In total, we generated WGS data (150 base paired-end reads) for 20 individuals (Supplementary Table 1). Field sampling was conducted in 2017 and 2018 at several locations across Southern and Central Europe (Spain, France, Romania, and Hungary). Samples were hand-netted in the field, flash-frozen from live in a liquid nitrogen dry shipper (Voyageur 12) and stored at -70 $°C$. Wings were retained for identification. DNA extractions for all individuals were performed using a Qiagen DNeasy Blood & Tissue kit. Extractions were used to prepare TruSeq Nano gel-free libraries by Edinburgh Genomics which were sequenced on a NovaSeq 6000 or HiSeq X (Supplementary Table 1). Raw reads are deposited at the ENA (accession number PRJEB76171).

QC, read mapping, variant calling, and summaries

Reads were trimmed and checked for quality using `FastQC v0.11.8` (Andrews, 2016) both before and after trimming with `FastP v0.20.0` (Chen et al., 2018), using `MultiQC v1.7` (Ewels et al., 2016) to visualise the results. Trimmed reads were aligned to the *I. podalirius* reference assembly (Mackintosh et al., 2022) using `bwa-mem v0.7.17` (Li, 2013). We marked duplicates using `sambamba v0.6.6` (Tarasov et al., 2015). Variants were called using `freebayes v1.3` (Garrison and Marth, 2012) `(-k -w -j -T 0.02 -E -1 --report-genotype-likelihood-max)`. A principle components analysis (PCA) was performed on intergenic autosomal variants using `plink v1.9` (Purcell et al., 2007). Genetic diversity (π), mean individual heterozygosity (H) and divergence (d_{XY}) were estimated at intergenic sites using the ***gIMble*** 'gimbleprep' module (Laetsch et al., 2023).

Fitting models of speciation across the genome using the bSFS

To infer the likely speciation history of this species pair and to estimate migration rates along the genome we used the software package ***gIMble*** (Laetsch et al., 2023). This analysis was restricted to the non-HZ set of individuals. As the inference assumes that each sample contributes diploid genotypes, analysis was restricted to the autosomes to allow the inclusion of both male and female data. Demographic models fit by ***gIMble*** assume a neutral model of evolution, and so we focused analysis on intergenic sequence (39% of the assembly), i.e. genic and repeat-rich regions and contigs that were not scaffolded into chromosomes were excluded. We filtered genotype (GT) calls to a

minimum depth of eight reads per sample and a maximum depth of three times the mean coverage per sample. Additionally, GT calls were required to have a minimum PHRED quality of one and SNPs within 2 bases of indels were removed. We used the `gIMble` 'parse' module to quantify genetic diversity and divergence for the filtered subset of the data. We summarised variation in pair-blocks of 64 bases and tallied all blockwise site frequency configurations of mutations across heterospecific sample pairs (see Laetsch et al. (2023) for details). We then fitted 'strict divergence' (DIV) and 'isolation with migration' (IM) demographic models to the genome-wide blockwise site frequency spectrum using the `gIMble` 'optimize' module.

To quantify heterogeneity in m_e and N_e, we fit a grid of parameters to sliding windows of a fixed length of 28,125 (pair-blocks) with a 20% overlap along the genome. This results in a total of 14,173 windows with a minimum span of 50 kb. The grid discretised N_e from 100,000 to 1,500,000 (in increments of 100,000) for *I. feisthamelii* from 100,000 to 900,000 (in increments of 50,000) for *I. podalirius* and from 100,000 to 2,400,000 (in increments of 100,000) for the ancestral population; m_e (forwards in time from *I. feisthamelii* into *I. podalirius*) was discretised from 0 to 4e-7, in increments of 5e-9. The split time T was fixed to the global result of 2,181,320 generations (Table 2) and the mutation rate was set to $\mu = 2.9 \times 10^{-9}$ per base and generation (Keightley et al., 2014) throughout. We label windows as barriers to gene flow where the marginal support for a DIV model (i.e. $m_\mathrm{e} = 0$) is greater than the support for an IM model parameterised with the most likely inferred effective migration rate under a null model of m_e variation (i.e. $\Delta_{B,0} > 0$).

Simulations and bootstrapping

We used the following bootstrapping approach to test the global support for an IM model over a DIV model: we performed 100 simulations using `msprime` (Baumdicker et al., 2022) (via the `gIMble` 'simulate' module) parameterised by the DIV history which best fit the empirical data. We simulated 14,173 windows of the same size as the real data, i.e. 28,125 (64 base) pair-blocks, for six diploid individuals per population to match the empirical sample set. We simulated a discrete genome and an infinite allele mutation model. We assumed a constant per base crossover rate based of one crossover per male meiosis per chromosome (i.e. each chromosome has a sex-averaged map length of 25 cM) and a mutation rate of 2.9×10^{-9} per base and generation per base and generation, as estimated for *Heliconius* butterflies (Keightley et al., 2015). We fit a DIV model and an IM model to each simulation and compared the null distribution of relative fit ($\ln CL$) to the empirical $\ln CL$.

To adjust our barrier definition for false positives (which are expected at an appreciable rate when the background m_e is low), we ran a parametric bootstrap on the local estimates m_e: for each window, we simulated 100 replicates under the best fitting local background history using ***msprime*** (Baumdicker et al., 2022) (via the ***gIMble*** 'simulate' module) and obtained a null distribution of $\Delta_{B,0}$. These simulations were analogous to the bootstrap for the global model, except that we allowed N_e parameters to vary between windows. We simulated under a null model with a globally fixed m_e, but accounted for variation in N_e by assuming the best composite log-likelihood N_e parameter inferred for each window. Only windows for which $\Delta_{B,0}$ in the real data was greater than the largest value contained in the $\Delta_{B,0}$ distribution from simulated data were labelled as barriers. This ensures a false positive rate < 0.01.

To test whether various metrics are associated with barrier windows we used a simple resampling approach. In all instances, random empirical estimates of each per-window metric were sampled without replacement to generate datasets of sizes relevant to the scope of the resampling scheme. We compared the empirical estimate to the distribution of means of 1000 resampled data sets. Unless otherwise indicated, we resampled datasets with respect to each chromosome in a circularised fashion (similar to the shift-permutation approach outlined by Yassin et al. (2016) and Nouhaud et al. (2022)), by shifting the assignments of barrier windows within a chromosome irrespective of chromosome ends by a random integer. This approach accounts for between-chromosome variation in recombination rates and generates null distributions that have the same clustering as barriers inferred in the data. Finally, we repeated each circular bootstrap after excluding each of the HZ samples in turn to check for robustness to sub-sampling. For each of these tests we consider an adjusted significance threshold of $p = 0.05/6 \approx 0.008$. The bootstrapping was implemented using a custom script available at `https://github.com/LohseLab/circular_bootstrap`.

Estimating hybrid indices and the ancestry of hybrid zone individuals

We polarized all variable sites (across all individuals) that were not singletons (which are uninformative for genome polarisation by association in state) and estimated genome-wide hybrid indices (HIs) using the ***diem*** framework implemented in both R and Mathematica (Baird et al., 2023). Variants were subject to the same filtering criteria as the ***gIMble*** analysis. We calculated HIs per individual using sets of polarised sites with high diagnostic index (DI > -20). We used chromosome subsets of these sites to calculate HIs per chromosome. At a further reduction in scale we computed HI for each ***gIMble*** window and compared D across all individuals between barrier and non-barrier

gIMble windows using the bootstrap scheme described above.

Deconfounding signal from multiple barriers

diem is designed to polarise genomes with respect to one barrier at a time, however trial *diem* analysis of the full genomes dataset suggested two barriers were present in the data: the focal barrier to gene flow between 'French' *I. podalirius* and 'Iberian' *I. feisthamelii*, and a 'nuisance' barrier to geneflow between 'Iberian' and 'African' *I. feisthamelii*, presumably due to the Strait of Gibraltar. For the focal analysis, signal of the nuisance barrier was removed by censoring all sites with minority homozygous state only present in (the two) samples from north Africa.

Kernel smoothing of genotypes along chromosomes

diem estimates the polarity of each site independently. Where a barrier exists we may expect polarisation to reveal tracts of different inheritance along chromosomes. Downstream analyses of tract size distributions requires estimates of the boundaries of these tracts. We estimate tract boundaries using kernel smoothing of the diploid state along chromosomes. Working on the physical (Mb) metric, the Laplace distribution truncated at its 95% probability boundaries provides the kernel. This is centered on each site to provide a weighted average of states 'smoothed' over the chosen physical scale. The centre-site is then estimated to have the state with greatest weight. Where variable sites are dense on the physical metric, smoothed estimates will be influenced by many flanking sites, where sparse, few. Imposing a given smoothing kernel scale assumes we are uninterested in state variation at higher frequency (involving shorter tracts). The kernel smoothing is therefore being used as a low-pass signal filter to leave larger tracts with clearer boundaries.

Untangling blocks from genotypes

When diploid genomes are polarised with respect to a single barrier, an interval of heterozygous sites within otherwise homozygous chromosome genotype suggests a single tract of minority inheritance on one of the chromosome copies. While the same pattern would result from two minority tracts, one on each chromosome copy, that 'perfectly' abut (without overlap), simple genotypes can be parsimoniously (and automatically) parsed into haplotype tracts by assuming such perfect abutment is so rare as to be negligible. Complex genotypes, where multiple minority intervals occur, would require decisions regarding tract phase (whether or not the minority tracts occupy the same chromosome copy), if we wished to estimate tract size distributions of both minority and

majority tracts. However, comparison to theory for tract size distributions (Baird, 1995) requires only minority tract sizes: Then, no phasing decisions are necessary, only a decision regarding which barrier-side state is in the minority for an individual. This can be decided with little uncertainty using an estimate of the individual's HI taken over very many sites genome wide.

Acknowledgements

We would like to thank Carla and Oskar Lohse for catching the two most informative hybrid samples: individuals 1322 and 1325. This work was supported by a European Research Council starting grant (ModelGenomLand 757648) to KL which also supported DRL. SE was supported by an EastBio studentship from the British Biological Sciences Research Council (BBSRC). KL was supported by a fellowship from the Natural Environment Research Council (NERC, NE/L011522/1). RV was supported by Grant PID2019-107078GB-I00 funded by Ministerio de Ciencia e Innovación and Agencia Estatal de Investigación (MCIN/AEI/10.13039/501100011033). We thank Katy McDonald for help in the molecular lab, Alex Hayward for help with field collections and Edinburgh Genomics for generating libraries and sequence data. We are indebted to Vlad Dincă, Raluca Vodă and Leonardo Dapporto for contributing samples and to Nick Barton for helpful suggestions on the analyses of admixture tracts and Alex Mackintosh and three reviewers and the AE for insightful comments on an earlier version of this manuscript.

Compliance with ethical standards

Field sampling of butterflies was conducted in compliance with the School of Biological Sciences Ethics Committee at the University of Edinburgh and the ERC ethics review procedure. Permissions for field sampling were obtained from the Generalitat de Catalunya (SF/639), the Gobierno de Aragon (INAGA/500201/24/2018/0614 to Karl Wotton) and the Gobierno del Principado de Asturias (014252).

Data Availability Statement

Read data is available from the ENA at PRJEB76171. Reads for sample IP_504 were generated by a previous study (Mackintosh et al., 2022) and are available at the ENA at PRJEB51340. Data underlying plots and statistics can be found at https://github.com/samebdon/iphiclides_speciation_data.

APPENDIX

In the Appendix of Baird (1995, Equation A10), Barton expressed the per migrant contribution to the distribution of continuous tract length x for two infinite demes of coupling θ genomes, T rescaled generations after starting to exchange migrants, in terms of Kummer's confluent hypergeometric function ${}_1F_1\left(a;b;z\right)$ (Kummer, 1837):

$$F\left(x,T\right) = Te^{-x(1+\theta)T}{}_1F_1\left(\frac{\theta-1}{\theta+1};2;-T(1+\theta)(1-x)\right) \tag{A-1}$$

This can be re-arranged such that tract length only appears as an argument of the confluent hypergeometric function, not in the initial term, by using Kummer's first transformation:

$${}_1F_1\left(a;b;z\right) = e^z{}_1F_1\left(b-a;b;-z\right) \tag{A-2}$$

Applying transformation A-2 to the confluent hypergeometric function in A-1:

$${}_1F_1\left(\frac{\theta-1}{\theta+1};2;-T(1+\theta)(1-x)\right) = e^{-T(1+\theta)(1-x)}{}_1F_1\left(2-\frac{\theta-1}{\theta+1};2;T(1+\theta)(1-x)\right) \tag{A-3}$$

Multiplying both sides of A-3 by the initial term in A-1, and simplifying, tract length appears only in the confluent hypergeometric function:

$$F\left(x,T\right) = Te^{-T(1+\theta)}{}_1F_1\left(\frac{3+\theta}{1+\theta};2;T(1+\theta)(1-x)\right) \tag{A-4}$$

In this form of Barton's result the first argument of the confluent hypergeometric is the negative log-log gradient of the equilibrium distribution of tract length y from Barton (1983, Eq (5)), clarifying the link between Barton's time T and equilibrium solutions. Integrating contributions A-1 since time of contact, the distribution of tract lengths per migrant found in either infinite deme is:

$$\int_0^T F(x,t)dt = (1+\theta)^{-2}x^{-\frac{3+\theta}{1+\theta}};T \longrightarrow \infty \tag{A-5}$$

The left hand expression can be found by numerical integration for any time T, and becomes equal to the right hand equilibrium solution for progressively smaller tracts as time goes on.

References

Abbott, R., Albach, D., Ansell, S., Arntzen, J. W., Baird, S. J. E., Bierne, N., Boughman, J., Brelsford, A., Buerkle, C. A., Buggs, R., Butlin, R. K., Dieckmann, U., Eroukhmanoff, F., Grill, A., Cahan, S. H., Hermansen, J. S., Hewitt, G., Hudson, A. G., Jiggins, C., Jones, J., Keller, B., Marczewski, T., Mallet, J., Martinez-Rodriguez, P., Möst, M., Mullen, S., Nichols, R., Nolte, A. W., Parisod, C., Pfennig, K., Rice, A. M., Ritchie, M. G., Seifert, B., Smadja, C. M., Stelkens, R., Szymura, J. M., Väinölä, R., Wolf, J. B. W. and Zinner, D. (2013), 'Hybridization and speciation', *Journal of Evolutionary Biology* **26**(2), 229–246.
URL: *https://onlinelibrary.wiley.com/doi/abs/10.1111/j.1420-9101.2012.02599.x*

Aeschbacher, S., Selby, J. P., Willis, J. H. and Coop, G. (2017), 'Population-genomic inference of the strength and timing of selection against gene flow', *Proceedings of the National Academy of Sciences* **114**(27), 7061–7066.

Andrews, S. (2016), 'FastQC Version 0.11. 5', *A Quality Control Tool for High Throughput Sequence Data* .

Arnold, M. L., Sapir, Y. and Martin, N. H. (2008), 'Genetic exchange and the origin of adaptations: prokaryotes to primates', *Philosophical Transactions of the Royal Society B: Biological Sciences* **363**(1505), 2813–2820.

Bachtrog, D., Mahajan, S. and Bracewell, R. (2019), 'Massive gene amplification on a recently formed Drosophila Y chromosome', *Nature Ecology & Evolution* **3**(11), 1587–1597.

Baird, S. (1995), 'A simulation study of multilocus clines', *Evolution* **49**(6), 1038–1045.

Baird, S. J., Petružela, J., Jaroň, I., Škrabánek, P. and Martínková, N. (2023), 'Genome polarisation for detecting barriers to geneflow', *Methods in Ecology and Evolution* **14**(2), 512–528.

Bank, C., Bürger, R. and Hermisson, J. (2012), 'The limits to parapatric speciation: Dobzhansky–Muller incompatibilities in a continent–island model', *Genetics* **191**(3), 845–863.

Banker, S. E., Bonhomme, F. and Nachman, M. W. (2022), 'Bidirectional Introgression between *Mus musculus domesticus* and *Mus spretus*', *Genome Biology and Evolution* **14**(1). evab288.
URL: *https://doi.org/10.1093/gbe/evab288*

Barton, N. and Bengtsson, B. O. (1986), 'The barrier to genetic exchange between hybridising populations', *Heredity* **57**(3), 357–376.

Barton, N. H. (1983), 'Multilocus clines', *Evolution* pp. 454–471.

Barton, N. H. and Charlesworth, B. (1984), 'Genetic revolutions, founder effects, and speciation', *Annual Review of Ecology and Systematics* **15**(1), 133–164.

Barton, N. H. and Gale, K. S. (1993), Genetic Analysis of Hybrid Zones, *in* 'Hybrid Zones and the Evolutionary Process', Oxford University Press.
URL: *https://doi.org/10.1093/oso/9780195069174.003.0002*

Barton, N. H. and Hewitt, G. M. (1985), 'Analysis of hybrid zones', *Annual review of Ecology and Systematics* pp. 113–148.

Baumdicker, F., Bisschop, G., Goldstein, D., Gower, G., Ragsdale, A. P., Tsambos, G., Zhu, S., Eldon, B., Ellerman, E. C., Galloway, J. G. et al. (2022), 'Efficient ancestry and mutation simulation with msprime 1.0', *Genetics* **220**(3), iyab229.

Bhattacharyya, T., Reifova, R., Gregorova, S., Simecek, P., Gergelits, V., Mistrik, M., Martincova, I., Pialek, J. and Forejt, J. (2014), 'X chromosome control of meiotic chromosome synapsis in mouse inter-subspecific hybrids', *PLoS genetics* **10**(2), e1004088.

Buggs, R. (2007), 'Empirical study of hybrid zone movement', *Heredity* **99**(3), 301–312.

Bush, G. L. (1994), 'Sympatric speciation in animals: new wine in old bottles', *Trends in Ecology & Evolution* **9**(8), 285–288.

Campbell, C. R., Poelstra, J. and Yoder, A. D. (2018), 'What is speciation genomics? The roles of ecology, gene flow, and genomic architecture in the formation of species', *Biological Journal of the Linnean Society* **124**(4), 561–583.

Capblancq, T., Mavárez, J., Rioux, D. and Després, L. (2019), 'Speciation with gene flow: evidence from a complex of alpine butterflies (Coenonympha, Satyridae)', *Ecology and evolution* **9**(11), 6444–6457.

Charlesworth, B., Coyne, J. A. and Barton, N. H. (1987), 'The relative rates of evolution of sex chromosomes and autosomes', *The American Naturalist* **130**(1), 113–146.

Chen, S., Zhou, Y., Chen, Y. and Gu, J. (2018), 'fastp: an ultra-fast all-in-one FASTQ preprocessor', *Bioinformatics* **34**(17), i884–i890.

Coutsis, J. and Van Oorschot, H. (2011), 'Differences in the male and female genitalia between *Iphiclides podalirius* and *Iphiclides feisthamelii*, further supporting species status for the latter (Lepidoptera: Papilionidae)', *Phegea* **39**(1), 12–22.

Descimon, H. and Mallet, J. (2009), 'Bad species', *Ecology of butterflies in Europe* **500**(C), 219.

Dieckmann, U. and Doebeli, M. (1999), 'On the origin of species by sympatric speciation', *Nature* **400**(6742), 354–357.

Drès, M. and Mallet, J. (2002), 'Host races in plant–feeding insects and their importance in sympatric speciation', *Philosophical Transactions of the Royal Society of London. Series B: Biological Sciences* **357**(1420), 471–492.
URL: *https://royalsocietypublishing.org/doi/abs/10.1098/rstb.2002.1059*

Ebdon, S., Laetsch, D. R., Dapporto, L., Hayward, A., Ritchie, M. G., Dinc, V., Vila, R. and Lohse, K. (2021), 'The Pleistocene species pump past its prime: Evidence from European butterfly sister species', *Molecular Ecology* **30**(14), 3575–3589.

Ewels, P., Magnusson, M., Lundin, S. and Käller, M. (2016), 'MultiQC: summarize analysis results for multiple tools and samples in a single report', *Bioinformatics* **32**(19), 3047–3048.

Excoffier, L., Dupanloup, I., Huerta-Sánchez, E., Sousa, V. C. and Foll, M. (2013), 'Robust demographic inference from genomic and SNP data', *PLoS genetics* **9**(10), e1003905.

Feder, J. L., Egan, S. P. and Nosil, P. (2012), 'The genomics of speciation-with-gene-flow', *Trends in genetics* **28**(7), 342–350.

Fraïsse, C., Popovic, I., Mazoyer, C., Spataro, B., Delmotte, S., Romiguier, J., Loire, E., Simon, A., Galtier, N., Duret, L. et al. (2021), 'DILS: Demographic inferences with linked selection by using ABC', *Molecular Ecology Resources* **21**(8), 2629–2644.

Frayer, M. E. and Payseur, B. A. (2024), 'Do genetic loci that cause reproductive isolation in the lab inhibit gene flow in nature?', *Evolution* **78**(6), 1025–1038.
URL: *https://doi.org/10.1093/evolut/qpae044*

Garrigan, D., Kingan, S. B., Geneva, A. J., Andolfatto, P., Clark, A. G., Thornton, K. R. and Presgraves, D. C. (2012), 'Genome sequencing reveals complex speciation in the *Drosophila simulans* clade', *Genome Research* **22**(8), 1499–1511.

Garrison, E. and Marth, G. (2012), 'Haplotype-based variant detection from short-read sequencing', *arXiv preprint arXiv:1207.3907* .

Gaunet, A., Dinca, V. E., Dapporto, L., Montagud, S., Voda, R., Schär, S., Badiane, A., Font, E. and Vila, R. (2019), 'Two consecutive *Wolbachia*-mediated mitochondrial introgressions obscure taxonomy in Palearctic swallowtail butterflies (*Lepidoptera*, *Papilionidae*)', *Zoologica Scripta* .

Godart, J.-B. (1842), *Histoire naturelle des lépidoptères ou papillons de France*, Vol. 15, Méquignon-Marvis fils.

Gompert, Z. and Buerkle, C. (2012), 'bgc: Software for Bayesian estimation of genomic clines', *Molecular Ecology Resources* **12**(6), 1168–1176.

Gompert, Z., Mandeville, E. G. and Buerkle, C. A. (2017), 'Analysis of Population Genomic Data from Hybrid Zones', *Annual Review of Ecology, Evolution, and Systematics* **48**(Volume 48, 2017), 207–229.
URL: *https://www.annualreviews.org/content/journals/10.1146/annurev-ecolsys-110316-022652*

Gosset, C. and Bierne, N. (2013), 'Differential introgression from a sister species explains high F ST outlier loci within a mussel species', *Journal of Evolutionary Biology* **26**(1), 14–26.

Gower, G., Ragsdale, A. P., Bisschop, G., Gutenkunst, R. N., Hartfield, M., Noskova, E., Schiffels, S., Struck, T. J., Kelleher, J. and Thornton, K. R. (2022), 'Demes: a standard format for demographic models', *Genetics* p. iyac131.
URL: *https://doi.org/10.1093/genetics/iyac131*

Grainger Hunt, W. and Selander, R. K. (1973), 'Biochemical genetics of hybridisation in European house mice', *Heredity* **31**(1), 11–33.

Hagberg, L., Celemín, E., Irisarri, I., Hawlitschek, O., Bella, J. L., Mott, T. and Pereira, R. J. (2022), 'Extensive introgression at late stages of species formation: Insights from grasshopper hybrid zones', *Molecular Ecology* **31**(8), 2384–2399.

Harris, K. and Nielsen, R. (2016), 'The Genetic Cost of Neanderthal Introgression', *Genetics* **203**(2), 881–891.
URL: *https://doi.org/10.1534/genetics.116.186890*

Harrison, R. G. et al. (1990), 'Hybrid zones: windows on evolutionary process.', *Oxford Surveys in Evolutionary Biology* **7**, 69–128.

Hedrick, P. W. (2013), 'Adaptive introgression in animals: examples and comparison to new mutation and standing variation as sources of adaptive variation', *Molecular Ecology* **22**(18), 4606–4618.

Hewitt, G. M. (1988), 'Hybrid zones-natural laboratories for evolutionary studies', *Trends in Ecology & Evolution* **3**(7), 158–167.

Hirase, S., Yamasaki, Y. Y., Sekino, M., Nishisako, M., Ikeda, M., Hara, M., Merilä, J. and Kikuchi, K. (2021), 'Genomic evidence for speciation with gene flow in broadcast spawning marine invertebrates', *Molecular Biology and Evolution* **38**(11), 4683–4699.

Iasi, L. N. M., Chintalapati, M., Skov, L., Bossoma Mesa, A., Hajdinjak, M., Peter, B. M. and Moorjani, P. (2024), 'Neandertal ancestry through time: Insights from genomes of ancient and present-day humans', *bioRxiv* pp. 2024–05.

Johnson, E. A. and Miyanishi, K. (2008), 'Testing the assumptions of chronosequences in succession', *Ecology Letters* **11**(5), 419–431.

Keightley, P. D., Ness, R. W., Halligan, D. L. and Haddrill, P. R. (2014), 'Estimation of the Spontaneous Mutation Rate per Nucleotide Site in a *Drosophila melanogaster* Full-Sib Family', *Genetics* **196**(1), 313–320.

Keightley, P. D., Pinharanda, A., Ness, R. W., Simpson, F., Dasmahapatra, K. K., Mallet, J., Davey, J. W. and Jiggins, C. D. (2015), 'Estimation of the spontaneous mutation rate in *Heliconius melpomene*', *Molecular Biology and Evolution* **32**(1), 239–243.

Kingston, S. E., Parchman, T. L., Gompert, Z., Buerkle, C. and Braun, M. J. (2017), 'Heterogeneity and concordance in locus-specific differentiation and introgression between species of towhees', *Journal of Evolutionary Biology* **30**(3), 474–485.

Kruuk, L., Baird, S., Gale, K. and Barton, N. H. (1999), 'A comparison of multilocus clines maintained by environmental adaptation or by selection against hybrids', *Genetics* **153**(4), 1959–1971.

Kummer, E. E. (1837), 'De integralibus quibusdam definitis et seriebus infinitis.'.

Laetsch, D. R., Bisschop, G., Martin, S. H., Aeschbacher, S., Setter, D. and Lohse, K. (2023), 'Demographically explicit scans for barriers to gene flow using gIMble', *PLoS Genetics* **19**(10), e1010999.

Lafranchis, T., Delmas, S. and Mazel, R. (2015), 'Le contact *Iphiclides feisthamelii-I. podalirius*. Statut de ces deux taxons (Lepidoptera, Papilionidae)', *Revue de l'Association Roussillonnaise d'Entomologie* **24**(3), 111–132.

Lenormand, T. (2002), 'Gene flow and the limits to natural selection', *Trends in Ecology & Evolution* **17**(4), 183–189.

Li, H. (2013), 'Aligning sequence reads, clone sequences and assembly contigs with BWA-MEM', *arXiv preprint arXiv:1303.3997* .

Macholán, M., Baird, S. J., Dufková, P., Munclinger, P., Bímová, B. V. and Piálek, J. (2011), 'Assessing multilocus introgression patterns: a case study on the mouse X chromosome in central Europe', *Evolution* **65**(5), 1428–1446.

Macholán, M., Munclinger, P., Šugerková, M., Dufková, P., Bímová, B., Božíková, E., Zima, J. and Piálek, J. (2007), 'Genetic analysis of autosomal and X-linked markers across a mouse hybrid zone', *Evolution* **61**(4), 746–771.

Mackintosh, A., Laetsch, D. R., Baril, T., Ebdon, S., Jay, P., Vila, R., Hayward, A. and Lohse, K. (2022), 'The genome sequence of the scarce swallowtail, *Iphiclides podalirius*', *G3* **12**(9), jkac193.

Mackintosh, A., Vila, R., Laetsch, D. R., Hayward, A., Martin, S. H. and Lohse, K. (2023), 'Chromosome fissions and fusions act as barriers to gene flow between Brenthis fritillary butterflies', *Molecular Biology and Evolution* **40**(3), msad043.

Mailund, T., Halager, A. E., Westergaard, M., Dutheil, J. Y., Munch, K., Andersen, L. N., Lunter, G., Prüfer, K., Scally, A., Hobolth, A. et al. (2012), 'A new isolation with migration model along complete genomes infers very different divergence processes among closely related great ape species', *PLoS genetics* **8**(12), e1003125.

Mallet, J. (1986), 'Hybrid zones of *Heliconius* butterflies in Panama and the stability and movement of warning colour clines', *Heredity* **56**(2), 191–202.

Mank, J. E., Nam, K. and Ellegren, H. (2009), 'Faster-Z evolution is predominantly due to genetic drift', *Molecular Biology and Evolution* **27**(3), 661–670.

Martin, S. H., Dasmahapatra, K. K., Nadeau, N. J., Salazar, C., Walters, J. R., Simpson, F., Blaxter, M., Manica, A., Mallet, J. and Jiggins, C. D. (2013), 'Genome-wide evidence for speciation with gene flow in *Heliconius* butterflies', *Genome Research* **23**(11), 1817–1828.

Martin, S. H., Davey, J. W., Salazar, C. and Jiggins, C. D. (2019), 'Recombination rate variation shapes barriers to introgression across butterfly genomes', *PLoS Biology* **17**(2), e2006288.

Mather, K. (1938), 'Crossing-over', *Biological Reviews* **13**(3), 252–292.
URL: *https://onlinelibrary.wiley.com/doi/abs/10.1111/j.1469-185X.1938.tb00516.x*

Meier, J. I., Salazar, P. A., Kučka, M., Davies, R. W., Dréau, A., Aldás, I., Power, O. B., Nadeau, N. J., Bridle, J. R., Rolian, C., Barton, N. H., McMillan, W. O., Jiggins, C. D. and Chan, Y. F. (2021), 'Haplotype tagging reveals parallel formation of hybrid races in two butterfly species', *Proceedings of the National Academy of Sciences* **118**(25), e2015005118.
URL: *https://www.pnas.org/doi/abs/10.1073/pnas.2015005118*

Mérot, C., Salazar, C., Merrill, R. M., Jiggins, C. D. and Joron, M. (2017), 'What shapes the continuum of reproductive isolation? Lessons from *Heliconius* butterflies', *Proceedings of the Royal Society B: Biological Sciences* **284**(1856), 20170335.

Mondal, M., Bertranpetit, J. and Lao, O. (2019), 'Approximate Bayesian computation with deep learning supports a third archaic introgression in Asia and Oceania', *Nature Communications* **10**(1), 1–9.

Morán, T. and Fontdevila, A. (2014), 'Genome-wide dissection of hybrid sterility in *Drosophila* confirms a polygenic threshold architecture', *Journal of Heredity* **105**(3), 381–396.

Nadeau, N. J., Ruiz, M., Salazar, P., Counterman, B., Medina, J. A., Ortiz-Zuazaga, H., Morrison, A., McMillan, W. O., Jiggins, C. D. and Papa, R. (2014), 'Population genomics of parallel hybrid zones in the mimetic butterflies, *H. melpomene* and *H. erato*', *Genome Research* **24**(8), 1316–1333.

Ngeve, M. N., Van der Stocken, T., Sierens, T., Koedam, N. and Triest, L. (2017), 'Bidirectional gene flow on a mangrove river landscape and between-catchment dispersal of *Rhizophora racemosa* (Rhizophoraceae)', *Hydrobiologia* **790**(1), 93–108.

Nosil, P. (2008), 'Speciation with gene flow could be common', *Molecular Ecology* **17**(9), 2103–2106. **URL:** *https://onlinelibrary.wiley.com/doi/abs/10.1111/j.1365-294X.2008.03715.x*

Nosil, P., Funk, D. J. and Ortiz-Barrientos, D. (2009), 'Divergent selection and heterogeneous genomic divergence', *Molecular Ecology* **18**(3), 375–402.

Nouhaud, P., Martin, S. H., Portinha, B., Sousa, V. C. and Kulmuni, J. (2022), 'Rapid and predictable genome evolution across three hybrid ant populations', *PLOS Biology* **20**(12), 1–20. **URL:** *https://doi.org/10.1371/journal.pbio.3001914*

Näsvall, K., Boman, J., Höök, L., Vila, R., Wiklund, C. and Backström, N. (2023), 'Nascent evolution of recombination rate differences as a consequence of chromosomal rearrangements', *PLOS Genetics* **19**(8), 1–21.
URL: *https://doi.org/10.1371/journal.pgen.1010717*

Orr, H. A. (1995), 'The population genetics of speciation: the evolution of hybrid incompatibilities.', *Genetics* **139**(4), 1805–1813.
URL: *https://doi.org/10.1093/genetics/139.4.1805*

Otto, S. P. (2019), 'Evolutionary potential for genomic islands of sexual divergence on recombining sex chromosomes', *New Phytologist* **224**(3), 1241–1251.
URL: *https://nph.onlinelibrary.wiley.com/doi/abs/10.1111/nph.16083*

Papadopulos, A. S., Baker, W. J., Crayn, D., Butlin, R. K., Kynast, R. G., Hutton, I. and Savolainen, V. (2011), 'Speciation with gene flow on Lord Howe Island', *Proceedings of the National Academy of Sciences* **108**(32), 13188–13193.

Parchman, T., Gompert, Z., Braun, M. J., Brumfield, R., McDonald, D., Uy, J. A. C., Zhang, G., Jarvis, E., Schlinger, B. and Buerkle, C. (2013), 'The genomic consequences of adaptive divergence and reproductive isolation between species of manakins', *Molecular Ecology* **22**(12), 3304–3317.

Payseur, B. A. and Rieseberg, L. H. (2016), 'A genomic perspective on hybridization and speciation', *Molecular Ecology* **25**(11), 2337–2360.

Poikela, N. P., Laetsch, D. R., Kankare, M., Hoikkala, A. and Lohse, K. (2022), 'Experimental introgression in *Drosophila*: asymmetric postzygotic isolation associated with chromosomal inversions and an incompatibility locus on the X chromosome', *bioRxiv* .

Purcell, S., Neale, B., Todd-Brown, K., Thomas, L., Ferreira, M. A., Bender, D., Maller, J., Sklar, P., De Bakker, P. I., Daly, M. J. et al. (2007), 'PLINK: a tool set for whole-genome association and population-based linkage analyses', *The American Journal of Human Genetics* **81**(3), 559–575.

Racimo, F., Sankararaman, S., Nielsen, R. and Huerta-Sánchez, E. (2015), 'Evidence for archaic adaptive introgression in humans', *Nature Reviews Genetics* **16**(6), 359–371.

Ravinet, M., Faria, R., Butlin, R., Galindo, J., Bierne, N., Rafajlović, M., Noor, M., Mehlig, B. and Westram, A. (2017), 'Interpreting the genomic landscape of speciation: a road map for finding barriers to gene flow', *Journal of Evolutionary Biology* **30**(8), 1450–1477.

Reifová, R., Majerová, V., Reif, J., Ahola, M., Lindholm, A. and Procházka, P. (2016), 'Patterns of gene flow and selection across multiple species of Acrocephalus warblers: footprints of parallel selection on the Z chromosome', *BMC Evolutionary Biology* **16**(1), 1–12.

Remington, C. L. (1968), Suture-zones of hybrid interaction between recently joined biotas, *in* 'Evolutionary biology', Springer, pp. 321–428.

Rieseberg, L. H., Archer, M. A. and Wayne, R. K. (1999), 'Transgressive segregation, adaptation and speciation', *Heredity* **83**(4), 363–372.

Roux, C., Fraisse, C., Romiguier, J., Anciaux, Y., Galtier, N. and Bierne, N. (2016), 'Shedding light on the grey zone of speciation along a continuum of genomic divergence', *PLoS Biology* **14**(12), e2000234.

Saarman, N. P., Opiro, R., Hyseni, C., Echodu, R., Opiyo, E. A., Dion, K., Johnson, T., Aksoy, S. and Caccone, A. (2019), 'The population genomics of multiple tsetse fly (Glossina fuscipes fuscipes) admixture zones in Uganda', *Molecular Ecology* **28**(1), 66–85.

Sankararaman, S., Mallick, S., Dannemann, M., Prüfer, K., Kelso, J., Pääbo, S., Patterson, N. and Reich, D. (2014), 'The genomic landscape of Neanderthal ancestry in present-day humans', *Nature* **507**(7492), 354–357.

Schumer, M., Xu, C., Powell, D. L., Durvasula, A., Skov, L., Holland, C., Blazier, J. C., Sankararaman, S., Andolfatto, P., Rosenthal, G. G. and Przeworski, M. (2018), 'Natural selection interacts with recombination to shape the evolution of hybrid genomes', *Science* **360**(6389), 656–660. **URL:** *https://www.science.org/doi/abs/10.1126/science.aar3684*

Stankowski, S. and Ravinet, M. (2021), 'Defining the speciation continuum', *Evolution* **75**(6), 1256–1273.

Stankowski, S., Shipilina, D. and Westram, A. M. (2021), 'Hybrid Zones', *eLS* **2**, 1–12.

Stapley, J., Feulner, P. G., Johnston, S. E., Santure, A. W. and Smadja, C. M. (2017), 'Variation in recombination frequency and distribution across eukaryotes: patterns and processes', *Philosophical Transactions of the Royal Society B: Biological Sciences* **372**(1736), 20160455.

Szymura, J. M. and Barton, N. H. (1986), 'Genetic analysis of a hybrid zone between the fire-bellied toads, *Bombina bombina* and *B. variegata*, near Cracow in southern Poland', *Evolution* **40**(6), 1141–1159.

Tarasov, A., Vilella, A. J., Cuppen, E., Nijman, I. J. and Prins, P. (2015), 'Sambamba: fast processing of NGS alignment formats', *Bioinformatics* **31**(12), 2032–2034.

Taylor, C., Touré, Y. T., Carnahan, J., Norris, D. E., Dolo, G., Traoré, S. F., Edillo, F. E. and Lanzaro, G. C. (2001), 'Gene flow among populations of the malaria vector, *Anopheles gambiae*, in Mali, West Africa', *Genetics* **157**(2), 743–750.

Taylor, S. A., Curry, R. L., White, T. A., Ferretti, V. and Lovette, I. (2014), 'Spatiotemporally consistent genomic signatures of reproductive isolation in a moving hybrid zone', *Evolution* **68**(11), 3066–3081.

Taylor, S. A. and Larson, E. L. (2019), 'Insights from genomes into the evolutionary importance and prevalence of hybridization in nature', *Nature ecology & evolution* **3**(2), 170–177.

Teeter, K. C., Payseur, B. A., Harris, L. W., Bakewell, M. A., Thibodeau, L. M., O'Brien, J. E., Krenz, J. G., Sans-Fuentes, M. A., Nachman, M. W. and Tucker, P. K. (2008), 'Genome-wide patterns of gene flow across a house mouse hybrid zone', *Genome Research* **18**(1), 67–76.

Turelli, M. and Orr, H. A. (1995), 'The dominance theory of Haldane's rule.', *Genetics* **140**(1), 389–402.

Turner, L. M. and Harr, B. (2014), 'Genome-wide mapping in a house mouse hybrid zone reveals hybrid sterility loci and Dobzhansky-Muller interactions', *Elife* **3**, e02504.

Wang, R. L., Wakeley, J. and Hey, J. (1997), 'Gene flow and natural selection in the origin of *Drosophila pseudoobscura* and close relatives', *Genetics* **147**(3), 1091–1106.

Westram, A. M., Faria, R., Johannesson, K. and Butlin, R. (2021), 'Using replicate hybrid zones to understand the genomic basis of adaptive divergence', *Molecular Ecology* **30**(15), 3797–3814.

Wiemers, M. (2003), Chromosome differentiation and the radiation of the butterfly subgenus Agrodiaetus (Lepidoptera: Lycaenidae: Polyommatus): a molecular phylogenetic approach, PhD thesis, Bonn, Univ., Diss., 2003.

Wiemers, M. and Fiedler, K. (2007), 'Does the DNA barcoding gap exist?–a case study in blue butterflies (Lepidoptera: Lycaenidae)', *Frontiers in Zoology* **4**(1), 1–16.

Wiemers, M. and Gottsberger, B. (2010), 'Discordant patterns of mitochondrial and nuclear differentiation in the Scarce Swallowtail *Iphiclides podalirius feisthamelii* (Duponchel, 1832)(Lepidoptera: Papilionidae)', *Entomologische Zeitschrift* **120**(3), 111–115.

Wilkinson-Herbots, H. M. (2008), 'The distribution of the coalescence time and the number of pairwise nucleotide differences in the "isolation with migration" model', *Theoretical Population Biology* **73**(2), 277–288.

Wu, C.-I. (2001), 'The genic view of the process of speciation', *Journal of Evolutionary Biology* **14**(6), 851–865.

Yan, J., Zhu, M., Liu, W., Xu, Q., Zhu, C., Li, J. and Sang, T. (2016), 'Genetic variation and bidirectional gene flow in the riparian plant *Miscanthus lutarioriparius*, across its endemic range: implications for adaptive potential', *GCB Bioenergy* **8**(4), 764–776.
URL: *https://onlinelibrary.wiley.com/doi/abs/10.1111/gcbb.12278*

Yang, W., Feiner, N., Laakkonen, H., Sacchi, R., Zuffi, M. A., Scali, S., While, G. M. and Uller, T. (2020), 'Spatial variation in gene flow across a hybrid zone reveals causes of reproductive isolation and asymmetric introgression in wall lizards', *Evolution* **74**(7), 1289–1300.

Yassin, A., Debat, V., Bastide, H., Gidaszewski, N., David, J. R. and Pool, J. E. (2016), 'Recurrent specialization on a toxic fruit in an island Drosophila population', *Proceedings of the National Academy of Sciences* **113**(17), 4771–4776.

Supplementary materials

Supplementary figures

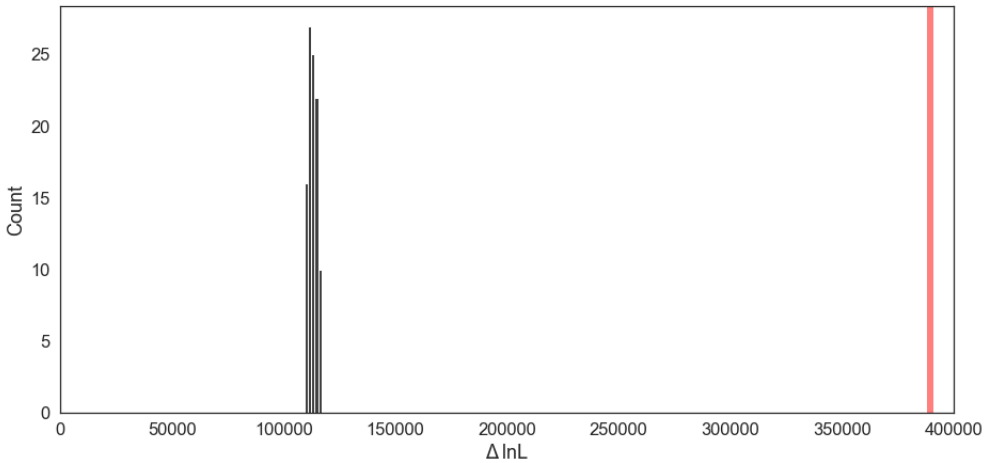

Figure S1 – The distribution of differences in log-likelihood ($\ln L$) between an isolation with migration (IM) model versus a model of strict divergence (DIV) fit to 100 replicates of data simulated under the best fitting empirical DIV model (black) and the empirical $\ln L$ (red). The improvement in fit of an IM model is much greater in the empirical data than in the simulations. See methods for simulation details.

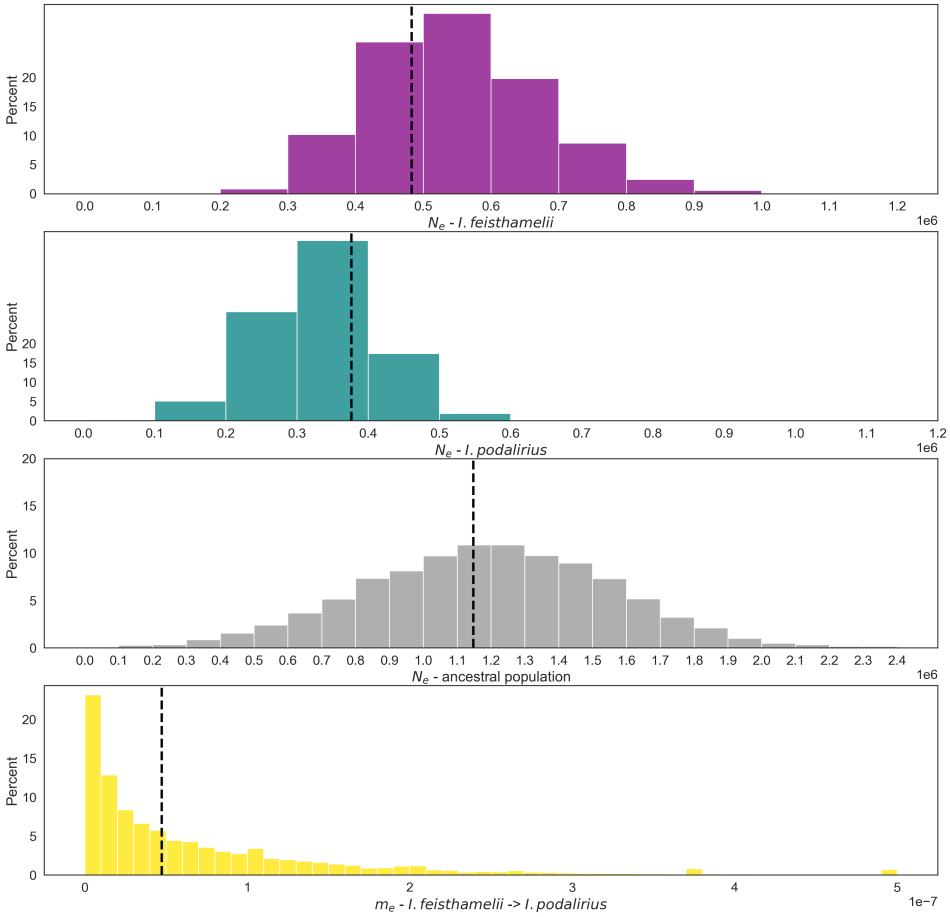

Figure S2 – The distributions of N_{fei} (purple), N_{pod} (teal), N_{anc} (grey), and $m_{e,i}$ (yellow) from *I. feisthamelii* into *I. podalirius* estimated in sliding windows using a 12x24x9x50 parameter grid. The vertical dashed lines indicate the global estimates of each parameter.

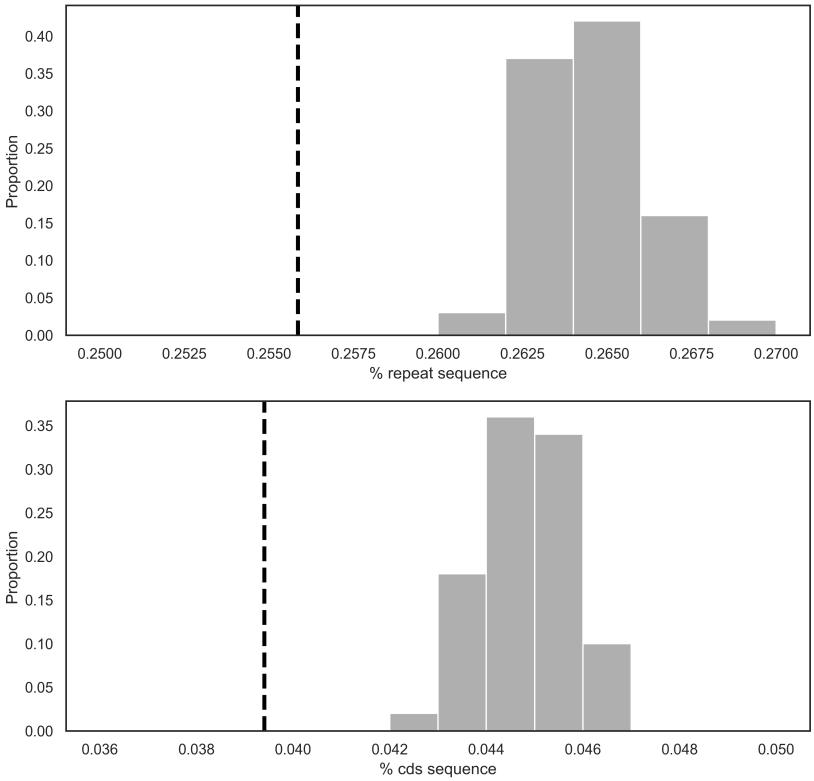

Figure S3 – The dashed lines indicate the mean density of repeats (top) and coding sequence (CDS) (bottom) in barrier regions defined via *gIMble*. Both are lower than the CDS and repeat proportion of data resampled at random using a circular resampling scheme.

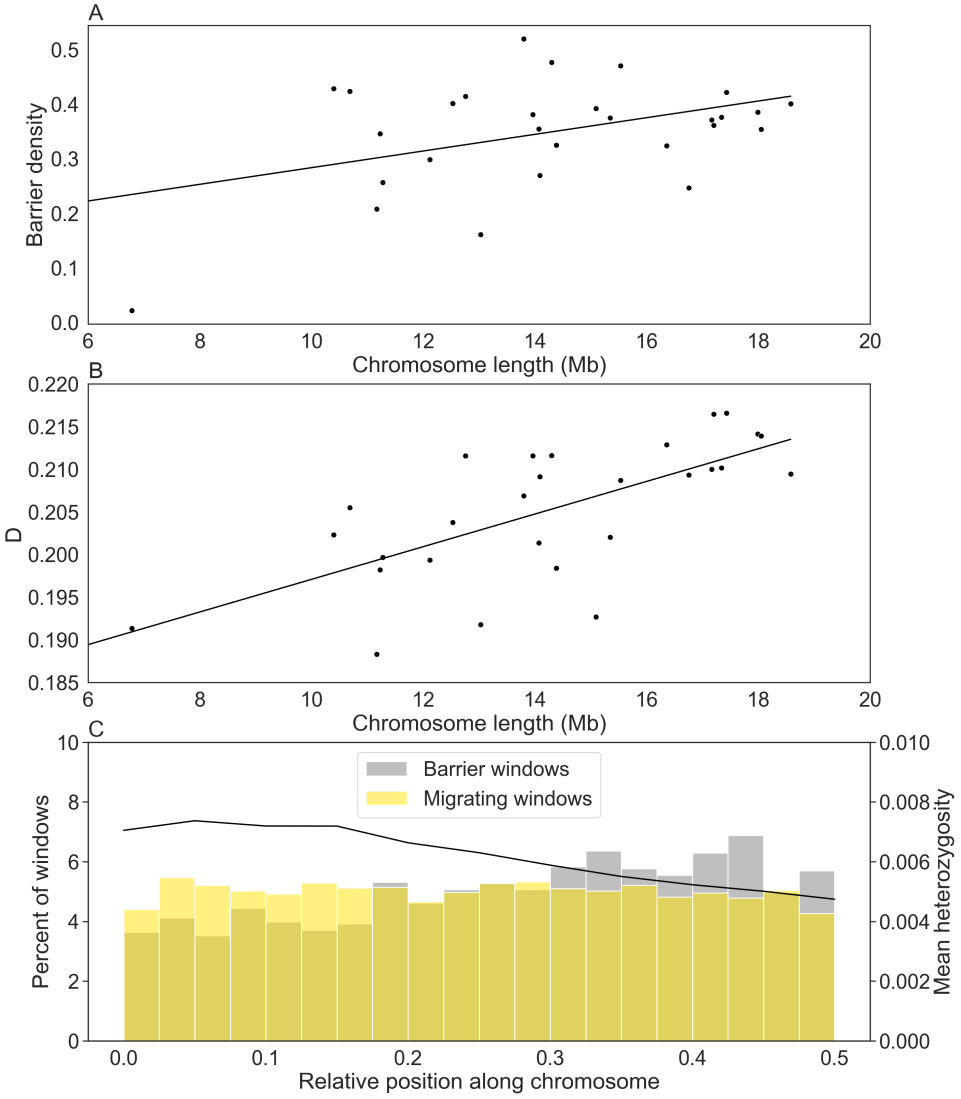

Figure S4 – A) Chromosome length (Mb) is positively correlated with barrier density (Pearson's $\rho = 0.425$, p = 0.0241). B) Chromosome length (Mb) is positively correlated with average D estimated within gIMble-defined windows (Pearson's $\rho = 0.74$, p = 4.84e-06). C) The distribution of relative positions from the telomeres (at 0) to chromosome centres (at 0.5) for `gIMble` barrier windows (grey) and non-barrier windows (yellow). The average heterozygosity for windows at different relative positions is shown by the black line. Barrier windows are further from the telomeres than non-barrier windows (circular bootstrap, p = 0.001).

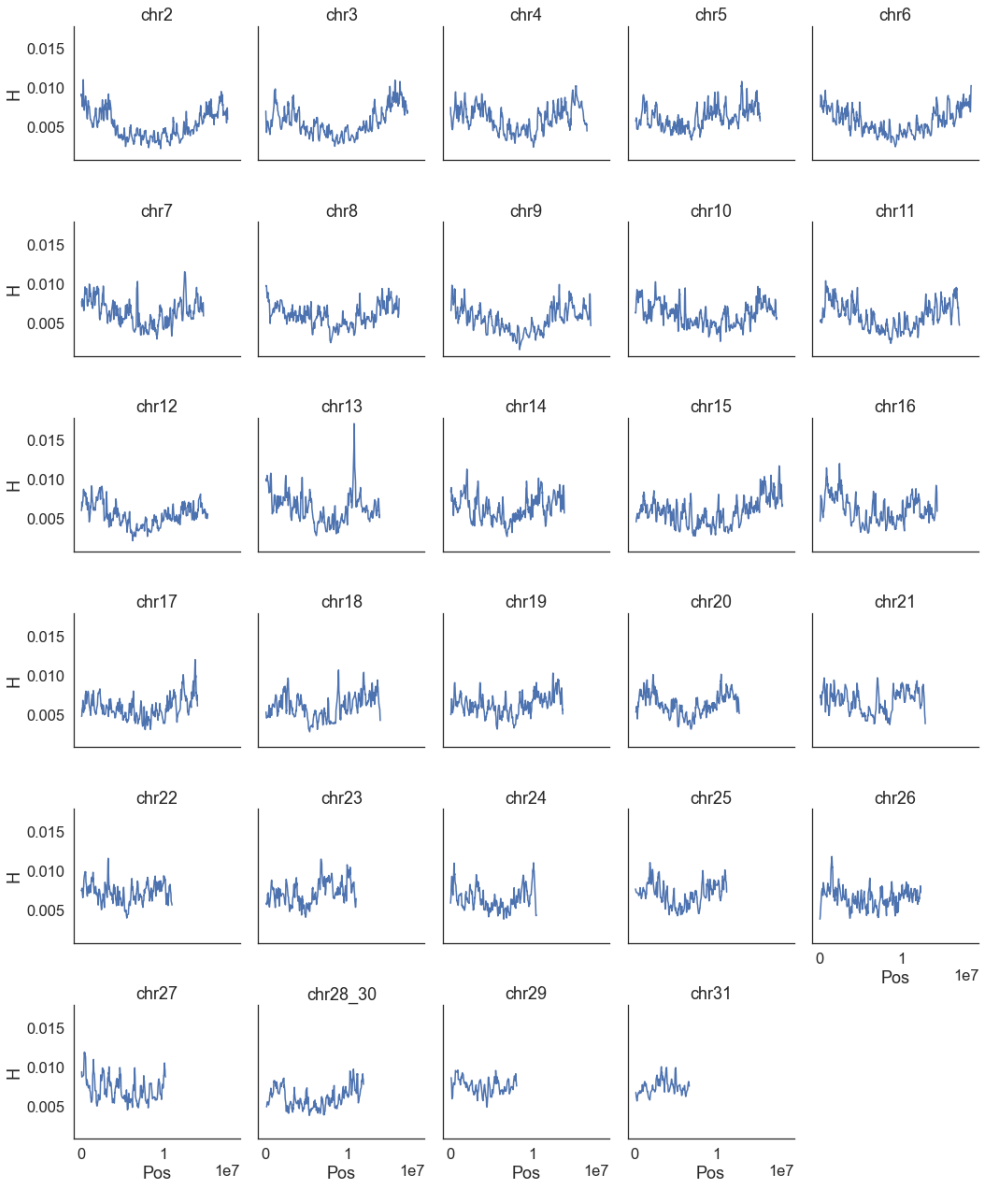

Figure S5 – Mean heterozygosity (H) in sliding windows of minimum 50kb across all chromosomes.

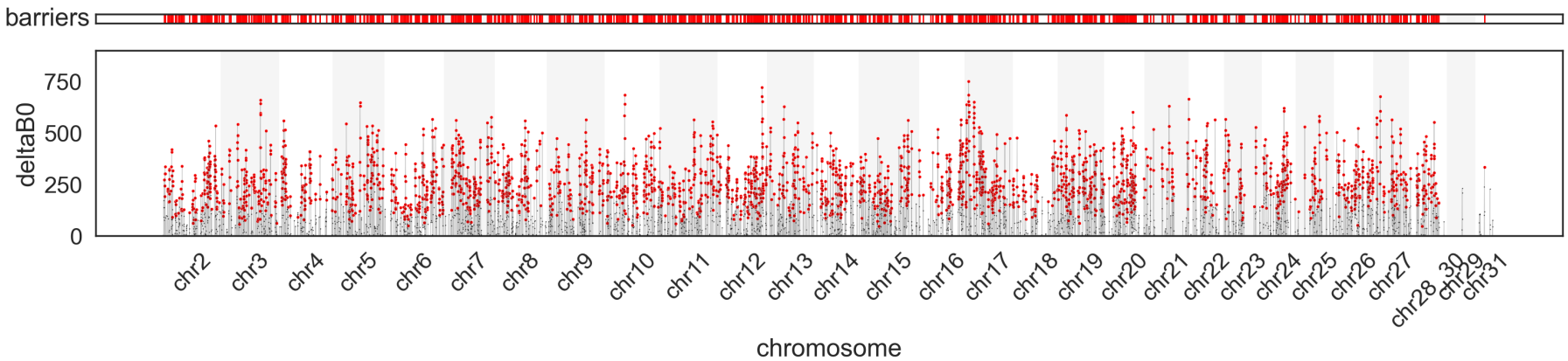

Figure S6 – Barriers to gene flow between *I. feisthamelii* and *I. podalirius*. The red bars in the top panel highlight the location of barrier windows. The bottom panel shows for each `gIMble` window, the difference in $\ln CL$ of $m_{\mathrm{e,i}} = 0$ from the background $m_{\mathrm{e}} = 1e-7$, $\Delta_{B,0}$. In windows where $\Delta_{B,0} > 0$, a model of strict divergence is more likely than an IM model. We highlight these barrier windows in red.

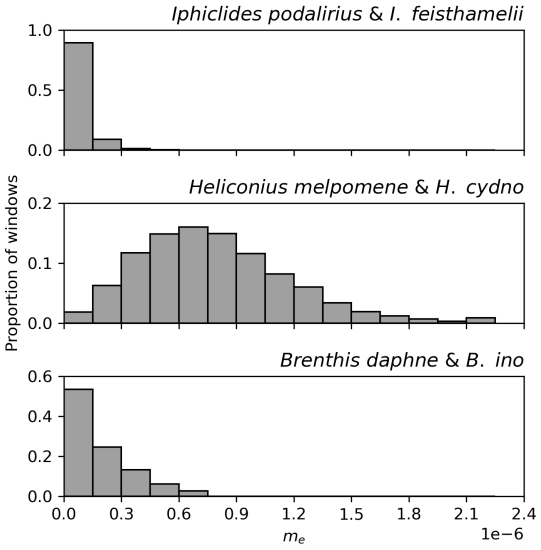

Figure S7 – The distribution of effective migration rates (m_e) between three pairs of butterfly sister species inferred by fitting IM models in windows across the genome. The rate of gene flow between *Iphiclides podalirius* and *I. feisthamelii* is lower than between *Heliconius melpomene* and *H. cydno* (Laetsch et al., 2023) and between *Brenthis daphne* and *B. ino* (Mackintosh et al., 2023).

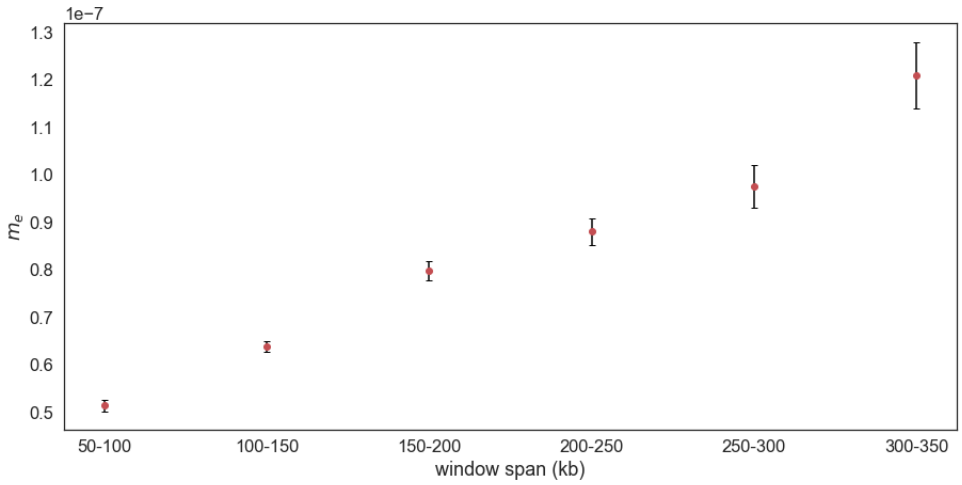

Figure S8 – Mean effective migration rates and standard errors for windows spanning different map lengths. Inferred migration rates are higher in windows spanning broader map lengths.